HHS Public Access

Author manuscript

J Med Chem. Author manuscript; available in PMC 2020 June 26.

Published in final edited form as:

J Med Chem. 2020 February 13; 63(3): 1216–1232. doi:10.1021/acs.jmedchem.9b01566.

Discovery of Potent and Selective Epidermal Growth Factor Receptor (EGFR) Bifunctional Small-Molecule Degraders

Meng Cheng[#],
University of North Carolina at Chapel Hill, Chapel Hill, North Carolina

Xufen Yu[#]
Icahn School of Medicine at Mount Sinai, New York, New York

Kaylene Lu, **Ling Xie**, **Li Wang**
University of North Carolina at Chapel Hill, Chapel Hill, North Carolina

Fanye Meng
Icahn School of Medicine at Mount Sinai, New York, New York

Xiaoran Han, **Xian Chen**
University of North Carolina at Chapel Hill, Chapel Hill, North Carolina

Jing Liu,
Icahn School of Medicine at Mount Sinai, New York, New York

Yue Xiong,
University of North Carolina at Chapel Hill, Chapel Hill, North Carolina

Jian Jin
Icahn School of Medicine at Mount Sinai, New York, New York

Abstract

Several epidermal growth factor receptor (EGFR) tyrosine kinase inhibitors have been developed and approved by Food and Drug Administration for the treatment of non-small-cell lung cancers, but their efficacy can be compromised by acquired drug resistance conferred by *EGFR*-mutant variants. Here, we described the discovery of a novel E3 ligase von Hippel–Lindau-recruiting EGFR degrader, MS39 (compound 6), and a first-in-class E3 ligase cereblon-recruiting EGFR degrader, MS154 (compound 10), using the proteolysis targeting chimera technology. These compounds potently induced the degradation of mutant but not wild-type EGFR in an E3 ligase-dependent manner in cancer cell lines and effectively suppressed the growth of lung cancer cells

Corresponding Authors Xufen Yu, xufen.yu@mssm.edu, **Yue Xiong**, yxiong@email.unc.edu, **Jian Jin**, jian.jin@mssm.edu.
[#]M.C. and X.F. contributed equally to this work.

ASSOCIATED CONTENT

Supporting Information

The Supporting Information is available free of charge at https://pubs.acs.org/doi/10.1021/acs.jmedchem.9b01566.

^{1}H NMR, ^{13}C NMR, and HPLC spectra of compounds **6**, **10**, **27**, and **28**; ^{1}H NMR and HPLC spectra of compounds **1–5** and **7–9**; illustration of binding of gefitinib to the EGFR kinase domain based on the cocrystal structure of the EGFR kinase domain in complex with gefitinib (PDB: 4I22); and expression levels of VHL and CRBN in HCC-827 (EGFR e19d), H3255 (EGFR L858R), OVCAR-8 (EGFR WT), and H1299 (EGFR WT) cells (PDF)

Molecular formula strings for all compounds (CSV)

The authors declare no competing financial interest.

compared with the corresponding negative controls. The global proteomic analyses revealed that the compounds were highly selective for EGFR. Furthermore, both compounds were bioavailable in mouse pharmacokinetic studies, and compound 6 is the first EGFR degrader suitable for in vivo efficacy studies. Overall, we provide a set of well-characterized chemical tools to the research community.

Graphical Abstract

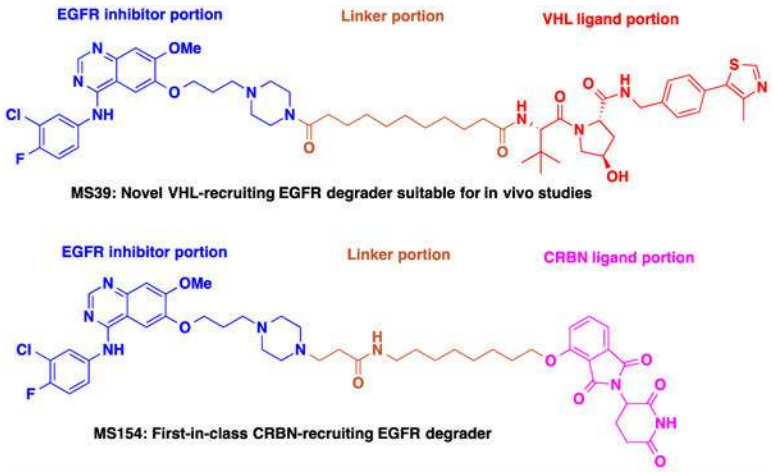

INTRODUCTION

Epidermal growth factor receptor (EGFR) is a transmembrane protein tyrosine kinase that functions as a receptor for members of the EGF family to trigger EGFR signal pathway in human epithelial cells, thereby regulating cell proliferation, invasion, metastasis, apoptosis, and angiogenesis.[1–3] Increased EGFR activity resulting from overexpression, mutation, or amplification of EGFR gene contributes to many human malignancies, including esophagus cancers, glioblastoma, anal cancers, epithelial cancers of the head and neck, breast cancers, and lung cancers, especially in non-small-cell lung cancers (NSCLCs).[1,4–6] Activating mutations, such as in-frame deletions of exon 19 and L858R mutation, which occur in the EGFR kinase adenosine triphosphate (ATP)-binding domain, have been categorized as the oncogenic driver in NSCLC.[1] Lung cancer is the leading cause of cancer death worldwide, and NSCLCs belong to the major category of lung cancers.[7] As a therapeutic target for NSCLC, EGFR has been extensively investigated by the biomedical community. In particular, studies on targeting the activity of mutant EGFR ATP-binding domain have led to the discovery of a number of Food and Drug Administration (FDA)-approved EGFR tyrosine kinase inhibitors (TKIs) (Figure 1). The first-generation TKIs gefitinib[8] and erlotinib[9] showed dramatic response initially and prolonged the survival in NSCLC patients. However, the secondary "gatekeeper" T790M mutation has increased the ATP-binding affinity and caused a relapse in most NSCLC patients after the 9–14 months of treatment.[10–13] To overcome the resistance, a number of the second-generation EGFR inhibitors targeting EGFR harboring T790M activating mutation have been developed, including afatinib and dacomitinib. The irreversible covalent bond with the Cys797 confers enhanced sensitivity and selectivity of these TKIs, but these drugs exhibited severe side effects due to

their activity against wild-type (WT) EGFR. Subsequently, the third-generation EGFR covalent inhibitors with improved selectivity over WT EGFR have been developed. However, C797S point mutation and/or other mechanisms have been shown to be associated with the acquired resistance to irreversible EGFR TKIs, which make NSCLC refractory to these inhibitors.[14–17] The fourth-generation EGFR TKIs such as EAI045[18] and other noncovalent inhibitors,[19–21] which target allosteric binding site(s), appear to be a major breakthrough against these tertiary mutations. Despite that, there is still an unmet medical need to develop novel small-molecule inhibitors or therapeutic approaches to overcome multipoint mutations of EGFR.[22]

As a potential therapeutic approach, proteolysis targeting chimeras (PROTACs) are capable of targeting a specific protein for degradation.[23–27] PROTACs are heterobifunctional molecules, typically consisting of a small molecule as the binder to the protein target of interest, a small-molecule ligand that recruits an E3 ligase, and a linker to conjugate the above two moieties.[28,29] The induced proximity by PROTACs leads to selective polyubiquitination of the target protein and its subsequent degradation at the proteasome. Unlike traditional enzyme inhibitors, which inhibit the catalytic activity of the target enzyme, PROTACs induce the degradation of its target protein, thus eliminating other functions of the protein in addition to its enzymatic activity. Moreover, while some kinase inhibitors are restricted to bind to the catalytic pocket,[30] PROTACs could potentially utilize all surface binding pockets on its target protein to achieve degradation. Thus, the emerging bifunctional small-molecule-mediated protein degradation paradigm could overcome the limitations of conventionally occupancy-driven inhibitors. Over the past several years, this technology has been successfully applied to the degradation of numerous proteins.[28,29,31–40] However, targeting membrane-bound receptors or receptor tyrosine kinases (RTKs) using this technology has not been extensively studied. Of note, the first successful EGFR PROTAC using a binder to the E3 ligase von Hippel–Lindau (VHL), PROTAC3, has recently been reported.[41]

Herein, we describe the design, synthesis, and characterization of a novel gefitinib-based VHL-recruiting EGFR degrader (**6**, MS39) that is more potent than the previously reported EGFR degrader PROTAC3 and a first-in-class gefitinib-based cereblon (CRBN)-recruiting EGFR degrader (**10**, MS154). We also developed two structurally similar compounds **27** (MS39N) and **28** (MS154N) that do not bind the corresponding E3 ligase as degrader negative controls for compounds **6** and **10**. We characterized these compounds in a battery of biochemical and cellular assays. In particular, we found that compounds **6** and **10** potently induced the degradation of mutant EGFR while sparing WT EGFR and inhibited cell proliferation more effectively than the degrader negative controls **27** and **28** in lung cancer cells. We also found that serum starvation enhanced the degradation effect, which might lead to improved effectiveness in tumors where serum deprivation is commonly observed. Our mechanism of action studies confirmed that the induced EGFR degradation was mediated by the corresponding E3 ubiquitin ligase. Importantly, our global proteomic analysis results indicate that compounds **6** and 10 are highly selective EGFR degraders. Moreover, compounds **6** and **10** were bioavailable in mouse pharmacokinetic (PK) studies. In particular, compound **6** is the first EGFR degrader with sufficient in vivo PK properties, thus

suitable for in vivo efficacy studies. Overall, we provide the research community a set of well-characterized chemical tools. Our study has also provided further evidence that RTKs such as EGFR can be targeted via the PROTAC technology and paved the way for further developing and exploring EGFR degraders as a potential therapeutic strategy for NSCLC and other cancers.

RESULTS AND DISCUSSION

Design, Synthesis, and Initial Evaluation of EGFR Bifunctional Small-Molecule Degraders.

Gefitinib (Figure 1), a highly potent and selective mutant EGFR TKI, has been approved since 2003 for the treatment of NSCLC.[42] It has been classified as a first-generation EGFR inhibitor. Gefitinib selectively binds the EGFR kinase domain, preventing ATP from binding and resulting in the inhibition of EGFR downstream signaling. While gefitinib binds WT EGFR with high affinity, it has a higher binding affinity for EGFR mutants compared to that of the WT.[10] We chose gefitinib as the binder to EGFR to develop EGFR bifunctional small-molecule degraders, mainly because of gefitinib's high binding affinity to mutant EGFR. The cocrystal structure of the EGFR kinase domain in complex with gefitinib (PDB ID: 4I22) indicates that the morpholine group of gefitinib projects the surface of the binding pocket (Supporting Information Figure S1). We therefore replaced the solvent-exposed morpholine group with a piperazine group and used the outer nitrogen of the piperazine group as the tethering site. We designed and synthesized a set of putative EGFR degraders by linking this piperazine moiety to VHL-1, which binds the E3 ligase VHL,[29] and pomalidomide/thalidomide, which bind the E3 ligase CRBN,[28] through several linkers (Figure 2).

Synthetic routes for preparing compounds **1–10** are outlined in Scheme 1. A simple nucleophilic substitution reaction between commercially available FAAH-IN-2 (**11**) and *tert*-butyl 4-(3-bromopropyl)piperazine-1-carboxylate (**12**),[43] followed by a deprotection reaction, produced intermediate **13**, which was subsequently converted to intermediate **14** via a straightforward two-step sequence. Intermediates **15–20** were prepared by amide-coupling reactions of VHL-1[29] with commercially available dicarboxylic acids. The canonical amide coupling of intermediate **13** with intermediates **15–20** afforded the desired compounds **1–6**. Compounds **7–9** were synthesized following the same amide-coupling procedures between intermediate **14** and reported pomalidomide-based linkers **21–23**.[44,45] Intermediate **26** was obtained via a nucleophilic substitution reaction and subsequent deprotection reaction from the commercially available thalidomide analog **24** and *tert*-butyl (8-iodooctyl)carbamate (**25**), which was prepared according to reported procedures.[46] Finally, the amide-coupling reaction between intermediate **14** and amine intermediate **26** generated thalidomide-based compound **10**.

The effect of these bifunctional compounds on reducing EGFR protein levels in cells was assessed via Western blotting (Figure 3). We found that compounds **1–3**, which contain several poly(ethylene glycol) (PEG) linkers conjugated to VHL-1, induced EGFR protein degradation weakly in HCC-827 cells treated with the compounds at up to 1 μM concentrations for 16 h. Among the three all-carbon linkers (in compounds **4–6**) we

explored, the longest linker with nine methylene groups (in compound **6**) led to effective EGFR protein degradation even at 10 nM. Among the four CRBN-recruiting compounds we explored, compound **9**, which contains a linker with six methylene groups, was more effective at reducing EGFR protein levels than compounds **7–8**, which contain PEG linkers. Interestingly, compound **10**, which contains a longer carbon linker (eight methylene groups) and the thalidomide moiety instead of the pomalidomide moiety, was slightly more effective at reducing EGFR protein levels than compound **9**. We therefore selected compounds **6** and **10** for further characterization.

We also designed compounds **27** and **28** (Figure 4) as structurally similar negative controls for degraders **6** and **10**, respectively. Compound **27** contains a diastereoisomer of VHL-1, which is known to be incapable of binding the VHL E3 ligase,[47–49] while maintaining the same EGFR binding moiety and very similar physicochemical properties as degrader **6**. Similarly, compound **28** contains an extra methyl group on the glutarimide moiety of thalidomide, which is known to abrogate its ability to bind the E3 ligase CRBN,[50] while also maintaining the same EGFR binding motif and similar physicochemical properties as degrader **10**.

Synthetic routes for preparing compounds **27** and **28** are outlined in Scheme 2. Intermediate **31** was prepared by an amide-coupling reaction of compound **29**, a diastereoisomer of VHL-1, with undecanedioic acid (**30**). The canonical amide coupling of intermediate **13** with intermediate **31** afforded the desired compound **27**. Intermediate **33** was prepared by methylation of intermediate **32**, which was prepared according to the synthetic route in Scheme 1D, followed by the removal of the protecting group. Finally, an amide-coupling reaction between intermediate **14** and amine intermediate **33** furnished the target compound **28**.

Binding Affinities of Compounds 6, 10, 27, and 28 to WT and Mutant EGFR.

We next assessed the binding affinities of the parental inhibitor gefitinib, degraders **6** and **10**, and their negative controls **27** and **28** to EGFR WT and L858R mutants in a competitive binding assay (Figure 5).[51] Gefitinib displayed similar binding affinity to EGFR WT (K_d = 1.1 ± 2 nM) and L858R mutants (K_d = 0.8 ± 2 nM). Compared to gefitinib, the VHL-recruiting degrader **6** showed approximately 10-fold weaker binding affinities to EGFR WT (K_d = 11 ± 3 nM) and L858R mutants (K_d = 12 ± 7 nM). Interestingly, compared with gefitinib, the CRBN-recruiting degrader **10** preserved high binding affinity to EGFR WT (K_d = 1.8 ± 4 nM) but displayed a 5-fold weaker binding affinity to EGFR L858R mutant (K_d = 3.8 ± 5 nM). The negative control compounds **27** and **28** exhibited similar binding affinities to both EGFR WT and L858R mutants as degraders **6** and **10**. Overall, these compounds exhibited high binding affinities to both EGFR WT and L858R mutants, providing experimental evidence supporting our degrader and negative control design hypothesis that the linker and E3 ligand attachment at the solvent-exposed region do not significantly affect the binding of these compounds to EGFR.

Compounds 6 and 10 Potently Decrease EGFR Protein Level and Inhibit Downstream Signaling in Lung Cancer Cells.

To evaluate the effects of compounds 6 and 10 on degrading EGFR mutants and inhibiting downstream signaling, we chose two EGFR-mutant-bearing lung cancer cell lines that are highly sensitive to gefitinib, HCC-827 cells bearing an exon 19 deletion and H3255 cells bearing a L858R point mutation. The expression levels of both VHL and CRBN E3 ligases were confirmed in both cell lines (Supporting Information Figure S2). The effects of the compounds were assessed using combined Western blotting for the total EGFR protein level, autophosphorylation of EGFR, and downstream target AKT (Figure 6).

We first examined the EGFR protein degradation induced by compounds **6** and **10** in a wide range of concentrations. As illustrated in Figure 6, compounds **6** and **10** effectively reduced the mutant EGFR protein level in a concentration-dependent manner in both HCC-827 and H3255 cells. The maximum EGFR protein degradation was achieved over 95% when cells were treated with these two degraders at a concentration as low as 50 nM. Quantification of the Western blotting data determined that the DC_{50} values for compound **6** in HCC-827 and H3255 cells were 5.0 nM and 3.3 nM, respectively, with a 16 h treatment. The DC_{50} values of compound **10** were 11 nM and 25 nM, respectively. These results suggest that our degraders have a potent chemical knockdown effect. Consistent with previous reports,[52] we observed a slight "hook effect" in HCC-827 cells treated with both degraders at the highest concentration (10 μM), but this effect was undetectable in H3255 cells. Interestingly, the parental inhibitor gefitinib at 1 μM did not significantly reduce the EGFR protein level in HCC-827 cells but partially reduced the EGFR protein level in H3255 cells. It is unclear which factors are the main contributors to the observed difference. Nevertheless, gefitinib at 1 μM effectively inhibited the downstream signaling in both cell lines. Our degraders **6** and **10** also potently inhibited the EGFR autophosphorylation (p-EGFR) and AKT phosphorylation (p-AKT), which is a downstream target of EGFR signaling pathway, in both cell lines. It is worth to note that our EGFR degraders **6** and **10** did not affect the AKT protein levels in both cell lines. We observed that the VHL-recruiting degrader **6** displayed slightly better EGFR degradation and downstream signaling inhibition effects than the CRBN-recruiting degrader **10** in HCC-827 cells, and the difference was more significant in H3255 cells. We also performed a side-by-side comparison of our degraders **6** and **10** with the previously reported VHL-recruiting EGFR degrader PROTAC3.[41] The Western blotting results indicate that compound **6** and PROTAC3 displayed similar EGFR degradation and downstream signaling inhibition effects in both HCC-827 and H3255 cells. However, at high concentrations (e.g., 1 and 10 μM), PROTAC3 exhibited a much more significant hook effect than compounds **6** and **10** in both cell lines (Figure 6).

We next evaluated the effect of compounds **6** and **10** on inducing the degradation of the WT EGFR. We chose to use the ovarian cancer OVCAR-8 cell line and NSCLC H1299 cell line, which bear the WT EGFR, for the study. We first confirmed that both VHL and CRBN E3 ligases were expressed in these two cell lines (Supporting Information Figure S2). As illustrated in Figure 7, compounds **6** and **10** did not significantly reduce the WT EGFR protein levels in both OVCAR-8 and H1299 cells. This result is consistent with the previous finding that PROTAC3 did not degrade the WT EGFR.[41] It is unclear why compounds **6** and

10, as well as PROTAC3, selectively degrade EGFR mutants over the WT EGFR. This warrants further investigation.

We also evaluated the effect of compounds **27** and **28** on reducing EGFR protein levels in HCC-827 and H3255 cells. As expected, these designed negative controls, which do not bind the E3 ligases VHL and CRBN, did not significantly induce the degradation of EGFR mutants in both cell lines (Figure 8). The combination of high structural similarity (between compounds **27** and **28** and compounds **6** and **10**) and maintaining high binding affinity to WT and mutant EGFR (Figure 5) makes compounds **27** and **28** excellent negative controls for studying the degradation activity of compounds **6** and **10**. In addition, compared with compounds **6** and **10**, these two negative controls (**27** and **28**) displayed lower potency at inhibiting EGFR autophosphorylation (p-EGFR) and its downstream signaling (e.g., AKT phosphorylation (p-AKT)), suggesting that the pharmacological degradation of EGFR can enhance the inhibition of the downstream signaling.

We next performed time-course studies to assess the kinetics of the EGFR degradation and downstream signaling inhibition by compounds **6** and **10** in both HCC-827 and H3255 cells (Figure 9). In HCC-827 cells, compound **6** reduced the EGFR protein level substantially (~50%) after a 4 h treatment, while the robust inhibition of p-AKT was observed after a 1 h treatment. The near-complete degradation of the mutant EGFR by compound **6** was achieved around 12 h, and the complete degradation effect could sustain to 24 h. Compound **10** displayed a similar trend, reducing the half-maximum of the EGFR protein level after 3.5 h and achieving the maximum degradation after a 12 h treatment. In H3255 cells, compounds **6** and **10** reduced the EGFR protein level and inhibited downstream signaling also in a time-dependent manner and with similar kinetics. The rapid inhibition of p-AKT is most likely due to the inhibitory but not degradation activity of these compounds as they maintained high binding affinities to WT and mutant EGFR (Figure 5).

Solid tumor tissues often experience serum deprivation due to rapid proliferation and aberrant angiogenesis. We therefore opted to evaluate the effect of our degraders during serum starvation. As shown in Figure 10, degraders **6** and **10** showed a more pronounced effect on EGFR degradation after an 8 h treatment in a fetal bovine serum (FBS)-free medium in both HCC-827 and H3255 cells. It is unclear why serum starvation enhanced the degradation effect of these compounds. One plausible mechanism is that serum starvation may promote EGFR internalization,[53] which facilitates the degrader-mediated binding of the substrate EGFR to the cytoplasmic E3 ligases.

We next investigated the mechanism of action of compounds **6** and **10** in H3255 cells using a set of rescue assays (Figure 11A). Compared to DMSO control, a 2 h pretreatment of MLN4924,[54] an NEDD8-activating enzyme inhibitor that blocks cullins neddylation and hence inactivating cullin RING E3 ligases, blocked the EGFR degradation induced by compounds **6** and **10**. Pretreatment of cells with the VHL inhibitor VH-298,[55] negative control compound **27**, or parental EGFR inhibitor gefitinib also blocked the EGFR degradation induced by the VHL-recruiting degrader **6**. Similarly, pretreatment with the CRBN E3 ligase binder thalidomide,[50] negative control compound **28**, or gefitinib also blocked compound **10**'s EGFR degradation effect in H3255 cells. Taken together, these

results confirmed that the EGFR degradation effect induced by compounds **6** and **10** was mediated through the E3 ligase (VHL/CRBN)/ubiquitination pathway.

To assess the reversibility of the EGFR degradation effect induced by compounds **6** and **10**, we performed washout experiments. In HCC-827 cells, pretreated with compounds **6** and **10** for 12 h and washed with fresh medium, the protein level was recovered after 24 h (Figure 11B), indicating that the EGFR degradation effect mediated by compounds **6** and **10** is reversible. We also observed that p-EGFR was recovered after 24 h and p-AKT was recovered after 48 h. Similarly, the effect of compounds **6** and **10** on the EGFR degradation was reversible in H3255 cells. Interestingly, slightly prolonged EGFR degradation and EGFR autophosphorylation effects were observed in H3255 cells for both degraders, suggesting that HCC3255 cells might be more sensitive to compounds **6** and **10**.

Compounds 6 and 10 Inhibit Proliferation of Lung Cancer Cells.

We next evaluated cell growth inhibition effects of EGFR degraders in H3255 cells. The VHL-recruiting degrader **6** effectively inhibited the growth of H3255 cells and was significantly more potent than its control compound **27** (Figure 12), indicating that the cell growth inhibition effect of compound **6** is at least partially due to its EGFR degradation activity. Compound **6** was also more potent than the previously reported PROTAC3. The CRBN-recruiting degrader **10** also inhibited the growth of H3255 cell, albeit it was not as potent as compound **6** and PROTAC3. A potential contributor to the lower potency of compound **10** may be that compound **10** was less effective in degrading mutant EGFR than compound **6** and PROTAC3 in H3255 cells (Figure 6). Compared with the FDA-approved gefitinib, compounds **6** and **10** and PROTAC3 were less potent at cell growth inhibition, which is likely due to lower cell permeability of these degraders. Nevertheless, compounds **6** and **10** were more effective at inhibiting cell proliferation than their corresponding controls **27** and **28**. It is worth to note that these two pairs of compounds (compounds **6** and **27** and compounds **10** and **28**) have very similar physicochemical properties due to their very high structural similarities.

Compounds 6 and 10 Are Highly Selective EGFR Degraders.

To assess the selectivity of compounds 6 and 10 across the proteome, we performed the mass spectrometry (MS)-based label-free quantitative (LFQ) proteomics analysis in HCC-827 cells (Figure 13). A total of 57 unique peptides of EGFR were detected with over 50% sequence coverage. For EGFR, the log 2 ratio of LFQ intensity value for compound 6 or compound 10 treatment vs DMSO control was about –2 with the highest confidence among all identified proteins (4794 proteins from the compound 6 experiment and 4446 proteins from the compound 10 experiment). Over 75% of EGFR protein was degraded upon compound 6 or compound 10 treatment. The study also identified several other proteins being potentially downregulated after degrader treatment, but with lower fold change or confidence level. Overall, our global proteomic study results indicate that degraders 6 and 10 are highly selective for EGFR.

Compounds 6 and 10 Are Bioavailable in Mice.

We next assessed in vivo pharmacokinetic (PK) properties of degraders **6** and **10**. Each compound was administrated to six mice via a single intraperitoneal (IP) injection at a dose of 50 mg/kg. We were pleased to find that high plasma concentrations of compound **6** were achieved (Figure 14A). In particular, the high plasma concentrations (approximately 5 μM) were maintained over 8 h, and approximately 1 μM plasma concentration was achieved at 24 h post dosing. The high plasma concentrations and relatively long half-life of compound **6** are expected to be sufficient to induce EGFR degradation in vivo. To the best of our knowledge, compound **6** is the first EGFR degrader that has good in vivo PK properties and is suitable for in vivo efficacy studies. Compound **10** was also bioavailable in mice via IP injection, albeit the plasma concentrations of compound **10** decreased by about 10- to 100-fold in comparison to those of compound **6** (Figure 14B). The highest plasma concentration (approximately 500 nM) was achieved at 8 h post dosing for compound **10**. Importantly, both degraders were well tolerated, and no clinical signs were observed for the mice treated with either compound.

CONCLUSIONS

In summary, we have developed a novel gefitinib-based VHL-recruiting EGFR degrader (compound **6**) and a first-in-class gefitinib-based CRBN-recruiting EGFR degrader (compound **10**). Compounds **6** and **10** potently induced the degradation of EGFR mutants but not EGFR WT and inhibited the downstream signaling in cells. We conducted the mechanism of action studies, which confirmed that the effect of compounds **6** and **10** on EGFR degradation was mediated by the E3 ubiquitin ligases VHL and CRBN, respectively. Our kinetic and washout study results indicate that the EGFR degradation effect of compounds **6** and **10** has fast kinetics and is reversible. We also found that serum starvation enhanced the EGFR degradation effect of compounds **6** and **10**. In cell proliferation assays, compounds **6** and **10** effectively inhibited the growth of lung cancer cells. We also performed global proteomic analyses and found that compounds **6** and **10** were highly selective for EGFR. In addition, while both compounds **6** and **10** were bioavailable in mice, compound **6** is the first EGFR degrader that has sufficient in vivo PK properties and is suitable for in vivo efficacy studies. Furthermore, compound **6** was more potent than the previously reported VHL-recruiting EGFR degrader PROTAC3 in inhibiting the proliferation of lung cancer cells. Finally, we also developed compounds **27** and **28**, which do not bind the corresponding E3 ligase as degrader negative controls for compounds **6** and **10**. Compounds **27** and **28** maintained high binding affinities to WT and mutant EGFR, similar to compounds **6** and **10**, but did not induce EGFR degradation in cells. The very high structural similarities of compounds **27** and **28** with compounds **6** and **10** make compounds **27** and **28** excellent degrader negative controls for compounds **6** and **10**. Overall, degraders **6** and **10** and their negative controls **27** and **28** are well-characterized chemical tools, and we provide these tools to the research community for further investigating the roles of EGFR in pathophysiology. Further optimization of these EGFR degraders will likely result in improved lead compounds for exploring a potential novel therapeutic strategy for NSCLC and overcoming drug resistance. Finally, our study has also provided further evidence that the PROTAC technology can be applied to targeting RTKs.

EXPERIMENTAL SECTION

Chemistry General Procedures.

All chemical reagents were purchased from commercial vendors and used in syntheses without the need for further purification. A Teledyne ISCO Combi*Flash* Rf$^+$ instrument equipped with a variable wavelength UV detector and a fraction collector was used to conduct flash column chromatography. HP C18 Redi*Sep* Rf reverse-phase silica columns were also used for the purification of certain polar products. All compounds received final purification with preparative high-performance liquid chromatography (HPLC) on an Agilent Prep 1200 series with the UV detector set to 254 nm. Separation was performed at room temperature with a flow rate of 40 mL/min. Samples were injected into a Phenomenex Luna 750 × 30 mm, 5 μm C18 column, with the gradient program set to 10% of methanol (A) in H_2O containing 0.1% TFA (B) progressing to 100% of methanol or acetonitrile (A). All compounds assessed for biological activity were assured to have >95% purity after HPLC purification. HPLC spectra were obtained for all compounds using an Agilent 1200 series system with a DAD detector and a 2.1 mm × 150 mm Zorbax 300SB-C18 5 μm column for chromatography. Samples (0.5 μL) were injected onto a C18 column at room temperature, and the flow rate was set to 0.4 mL/min. Chromatography was performed with the solvents as follows: water containing 0.1% formic acid was designated as solvent A, while acetonitrile containing 0.1% formic acid was designated as solvent B. The linear gradient was set such that 1% B was used from 0 to 1 min, 1–99% B from 1 to 4 min, and 99% B from 4 to 8 min. High-resolution mass spectra (HRMS) data was acquired in positive ion mode using an Agilent G1969A API-TOF with an electrospray ionization (ESI) source. All compounds were also characterized using either a Bruker (Billerica, MA) DRX-600 NMR spectrometer (600 MHz, ^{1}H NMR) or a Bruker DXI 800 MHz spectrometer (800 MHz ^{1}H NMR, 201 MHz, ^{13}C NMR). Chemical shifts for all compounds are reported in units of parts per million (ppm, δ) relative to residual solvent peaks. ^{1}H NMR data are reported in the following format: chemical shift, multiplicity (s = singlet, d = doublet, t = triplet, q = quartet, m = multiplet), coupling constant, and integration.

(2S,4R)-1-((S)-2-(3-(3-(4-(3-((4-((3-Chloro-4-fluorophenyl)-amino)-7-methoxyquinazolin-6-yl)oxy)propyl)piperazin-1-yl)-3-oxopropoxy)propanamido)-3,3-dimethylbutanoyl)-4-hydroxy-N-(4-(4-methylthiazol-5-yl)benzyl)pyrrolidine-2-carboxamide (1).—To the solution of *N*-(3-chloro-4-fluorophenyl)-7-methoxy-6-(3-(piperazin-1-yl)propoxy)quinazolin-4-amine (**13**, 11.0 mg, 0.02 mmol) in DMSO (1 mL) were added 3-(3-(((*S*)-1-((2*S*,4*R*)-4-hydroxy-2-((4-(4-methylthiazol-5-yl)benzyl)carbamoyl) pyrrolidin-1-yl)-3,3-dimethyl-1-oxobutan-2-yl)amino)-3-oxopropoxy)propanoic acid (**15**, 11.5 mg, 0.02 mmol, 1.0 equiv), EDCI (6.0 mg, 0.03 mmol, 1.5 equiv), HOAt (4.2 mg, 0.03 mmol, 1.5 equiv), and NMM (6.1 mg, 0.06 mmol, 3.0 equiv). After being stirring overnight at room temperature, the resulting mixture was purified by preparative HPLC (10–100% methanol/0.1% TFA in H_2O) to afford the title compound **1** as white solid in TFA salt form (10.1 mg, 82% yield). ^{1}H NMR (600 MHz, CD_3OD) δ 8.91 (d, J = 4.0 Hz, 1H), 8.74 (s, 1H), 7.97 (d, J = 4.0 Hz, 1H), 7.95–7.85 (m, 2H), 7.69–7.62 (m, 1H), 7.50–7.33 (m, 4H), 7.26 (d, J = 4.1 Hz, 1H), 4.66 (td, J = 8.5, 7.6, 4.8 Hz, 1H), 4.59–4.44 (m, 3H), 4.43–4.29 (m, 4H), 4.07 (d, J = 4.2 Hz, 3H),

3.90 (d, J = 11.1 Hz, 1H), 3.83–3.55 (m, 11H), 3.50 (q, J = 7.5, 6.5 Hz, 2H), 2.80–2.60 (m, 2H), 2.54 (q, J = 5.5 Hz, 3H), 2.50–2.37 (m, 5H), 2.23 (dd, J = 13.6, 7.7 Hz, 1H), 2.07 (ddt, J = 13.5, 9.4, 4.6 Hz, 1H), 1.03 (s, 9H). HPLC 98% pure, t_R = 3.77 min; HRMS m/z [M + H]$^+$ calculated for $C_{50}H_{61}ClFN_9O_8S^+$ 1002.4109, found 1002.4141.

(2S,4R)-1-((S)-2-(tert-Butyl)-16-(4-(3-((4-((3-chloro-4-fluorophenyl)amino)-7-methoxyquinazolin-6-yl)oxy)propyl)-piperazin-1-yl)-4,16-dioxo-7,10,13-trioxa-3-azahexadecanoyl)-4-hydroxy-N-(4-(4-methylthiazol-5-yl)benzyl)pyrrolidine-2-carboxamide (2).—Compound **2** was prepared following the general procedure for preparing compound **1** from *N*-(3-chloro-4-fluorophenyl)-7-methoxy-6-(3-(piperazin-1-yl)propoxy)quinazolin-4-amine (**13**, 11.0 mg, 0.02 mmol) and (*S*)-15-((2*S*,4*R*)-4-hydroxy-2-((4-(4-methylthiazol-5-yl)benzyl)carbamoyl)pyrrolidine-1-carbonyl)-16,16-dimethyl-13-oxo-4,7,10-trioxa-14-azaheptadecanoic acid (16, 13.3 mg, 0.02 mmol). White solid (17.6 mg, 81% yield). ^{1}H NMR (600 MHz, CD_3OD) δ 8.98 (s, 1H), 8.74 (s, 1H), 7.99 (s, 1H), 7.93 (dd, J = 6.6, 2.7 Hz, 1H), 7.66 (ddd, J = 9.0, 4.2, 2.7 Hz, 1H), 7.51–7.33 (m, 5H), 7.28 (s, 1H), 4.64 (s, 1H), 4.60–4.46 (m, 4H), 4.40–4.33 (m, 3H), 4.08 (s, 3H), 3.89 (dd, J = 11.1, 4.3 Hz, 1H), 3.83–3.67 (m, 6H), 3.61 (pd, J = 10.7, 9.6, 5.6 Hz, 14H), 3.48 (t, J = 7.4 Hz, 2H), 2.62–2.50 (m, 2H), 2.50–2.39 (m, 7H), 2.22 (ddt, J = 11.9, 7.7, 2.1 Hz, 1H), 2.07 (ddt, J = 13.3, 9.0, 4.2 Hz, 1H), 1.03 (s, 9H). HPLC 98% pure, t_R = 4.89 min; HRMS m/z [M + H]$^+$ calculated for $C_{54}H_{70}ClFN_9O_{10}S^+$ 1090.4633, found 1090.4536.

(2S,4R)-1-((S)-2-(tert-Butyl)-22-(4-(3-((4-((3-chloro-4-fluorophenyl)amino)-7-methoxyquinazolin-6-yl)oxy)propyl)-piperazin-1-yl)-4,22-dioxo-7,10,13,16,19-pentaoxa-3-azadocosanoyl)-4-hydroxy-N-(4-(4-methylthiazol-5-yl)benzyl)pyrrolidine-2-carboxamide (3).—Compound **3** was prepared following the general procedure for preparing compound **1** from *N*-(3-chloro-4-fluorophenyl)-7-methoxy-6-(3-(piperazin-1-yl)propoxy)quinazolin-4-amine (**13**, 11.0 mg, 0.02 mmol) and (*S*)-19-((2*S*,4*R*)-4-hydroxy-2-((4-(4-methylthiazol-5-yl)benzyl)carbamoyl) pyrrolidine-1-carbonyl)-20,20-dimethyl-17-oxo-3,6,9,12,15-pentaoxa-18-azahenicosanoic acid (17, 15 mg, 0.02 mmol). White solid (9.5 mg, 40% yield). ^{1}H NMR (600 MHz, CD_3OD) δ 8.92 (s, 1H), 8.74 (s, 1H), 7.99 (s, 1H), 7.93 (dd, J = 6.6, 2.7 Hz, 1H), 7.66 (ddd, J = 8.9, 4.2, 2.6 Hz, 1H), 7.49–7.33 (m, 5H), 7.28 (s, 1H), 4.63 (s, 1H), 4.59–4.44 (m, 3H), 4.41–4.31 (m, 4H), 4.09 (s, 3H), 3.88 (d, J = 10.9 Hz, 1H), 3.83–3.66 (m, 6H), 3.66–3.52 (m, 22H), 3.49 (t, J = 7.4 Hz, 3H), 2.57 (ddd, J = 15.0, 7.3, 5.2 Hz, 1H), 2.51–2.38 (m, 7H), 2.22 (ddt, J = 11.7, 7.6, 2.0 Hz, 1H), 2.07 (ddd, J = 13.3, 9.2, 4.4 Hz, 1H), 1.03 (s, 9H). HPLC 99% pure, t_R = 3.81 min; HRMS m/z [M + H]$^+$ calculated for $C_{58}H_{78}ClFN_9O_{12}S^+$ 1178.5158, found 1178.5191.

(2S,4R)-1-((S)-2-(4-(4-(3-((4-((3-Chloro-4-fluorophenyl)amino)-7-methoxyquinazolin-6-yl)oxy)propyl)piperazin-1-yl)-4-oxobutanamido)-3,3-dimethylbutanoyl)-4-hydroxy-N-(4-(4-methylthiazol-5-yl)benzyl)pyrrolidine-2-carboxamide (4).—Compound **4** was prepared following the general procedure for preparing compound **1** from *N*-(3-chloro-4-fluorophenyl)-7-methoxy-6-(3-(piperazin-1-yl)propoxy)-quinazolin-4-amine (**13**, 11.0 mg, 0.02 mmol) and 4-(((*S*)-1-((2*S*,4*R*)-4-hydroxy-2-((4-(4-methylthiazol-5-yl)benzyl)carbamoyl) pyrrolidin-1-yl)-3,3-dimethyl-1-

oxobutan-2-yl)amino)-4-oxobutanoic acid (18, 10.6 mg, 0.02 mmol). White solid (9.0 mg, 47% yield). ^{1}H NMR (600 MHz, CD_3OD) δ 8.95 (s, 1H), 8.74 (s, 1H), 8.03–7.91 (m, 2H), 7.70–7.62 (m, 1H), 7.53–7.33 (m, 5H), 7.28 (s, 1H), 4.60 (d, J = 6.5 Hz, 1H), 4.58–4.46 (m, 2H), 4.46–4.30 (m, 4H), 4.09 (s, 5H), 3.95–3.74 (m, 2H), 3.70–3.39 (m, 4H), 2.84–2.55 (m, 6H), 2.55–2.39 (m, 6H), 2.22 (dd, J = 13.2, 7.7 Hz, 1H), 2.08 (ddd, J = 13.4, 9.2, 4.6 Hz, 2H), 1.04 (s, 9H). HPLC 96% pure, t_R = 4.99 min; HRMS m/z $[M + H]^+$ calculated for $C_{48}H_{58}ClFN_9O_7S^+$ 958.3847, found 958.3788.

(2S,4R)-1-((S)-2-(7-(4-(3-((4-((3-Chloro-4-fluorophenyl)amino)-7-methoxyquinazolin-6-yl)oxy)propyl)piperazin-1-yl)-7-oxoheptanamido)-3,3-dimethylbutanoyl)-4-hydroxy-N-(4-(4-methylthiazol-5-yl)benzyl)pyrrolidine-2-carboxamide (5).—Compound **5** was prepared following the general procedure for preparing compound **1** from *N*-(3-chloro-4-fluorophenyl)-7-methoxy-6-(3-(piperazin-1-yl)propoxy)-quinazolin-4-amine (**13**, 11.0 mg, 0.02 mmol) and 7-(((*S*)-1-((2*S*,4*R*)-4-hydroxy-2-((4-(4-methylthiazol-5-yl)benzyl)carbamoyl) pyrrolidin-1-yl)-3,3-dimethyl-1-oxobutan-2-yl)amino)-7-oxoheptanoic acid (19, 11.5 mg, 0.02 mmol). White solid (18.2 mg, 91% yield). ^{1}H NMR (600 MHz, CD_3OD) δ 8.94 (s, 1H), 8.74 (s, 1H), 8.00 (s, 2H), 7.94 (dd, J = 6.6, 2.7 Hz, 1H), 7.70–7.63 (m, 1H), 7.50–7.34 (m, 4H), 7.29 (d, J = 4.5 Hz, 1H), 4.64 (s, 1H), 4.61–4.46 (m, 2H), 4.46–4.32 (m, 3H), 4.08 (s, 5H), 3.90 (d, J = 11.0 Hz, 1H), 3.80 (dd, J = 10.9, 4.0 Hz, 1H), 3.48 (t, J = 7.3 Hz, 2H), 2.58–2.38 (m, 9H), 2.36–2.16 (m, 2H), 2.14–2.03 (m, 1H), 1.69–1.57 (m, 6H), 1.49–1.32 (m, 6H), 1.03 (s, 9H). HPLC 98% pure, t_R = 3.81 min; HRMS m/z $[M + H]^+$ calculated for $C_{51}H_{64}ClFN_9O_7S^+$ 1000.4316, found 1000.4342.

(2S,4R)-1-((S)-2-(11-(4-(3-((4-((3-Chloro-4-fluorophenyl)amino)-7-methoxyquinazolin-6-yl)oxy)propyl)piperazin-1-yl)-11-oxounde-canamido)-3,3-dimethylbutanoyl)-4-hydroxy-N-(4-(4-methylthiazol-5-yl)benzyl)pyrrolidine-2-carboxamide (6).—Compound **6** was prepared following the general procedure for preparing compound **1** from *N*-(3-chloro-4-fluorophenyl)-7-methoxy-6-(3-(piperazin-1-yl)-propoxy)quinazolin-4-amine (**13**, 11.0 mg, 0.02 mmol) and 11-(((*S*)-1-((2*S*,4*R*)-4-hydroxy-2-((4-(4-methylthiazol-5-yl)benzyl)-carbamoyl)pyrrolidin-1-yl)-3,3-dimethyl-1-oxobutan-2-yl)amino)-11-oxoundecanoic acid (20, 13.6 mg, 0.02 mmol). White solid (17.4 mg, 82% yield). ^{1}H NMR (800 MHz, CD_3OD) δ 9.12 (s, 1H), 8.76 (s, 1H), 8.02 (s, 1H), 7.96 (dd, J = 6.7, 2.7 Hz, 1H), 7.69 (dt, J = 7.4, 3.3 Hz, 1H), 7.49 (d, J = 7.8 Hz, 2H), 7.44 (d, J = 7.8 Hz, 2H), 7.36 (t, J = 8.9 Hz, 1H), 7.33 (s, 1H), 4.66 (s, 1H), 4.63–4.58 (m, 1H), 4.58–4.49 (m, 2H), 4.43–4.35 (m, 3H), 4.11 (s, 3H), 3.93 (d, J = 10.9 Hz, 1H), 3.83 (dd, J = 10.9, 4.0 Hz, 1H), 3.78–3.55 (m, 4H), 3.51 (t, J = 7.4 Hz, 2H), 3.37 (s, 2H), 3.30–2.97 (m, 4H), 2.56–2.41 (m, 7H), 2.33 (dt, J = 14.8, 7.6 Hz, 1H), 2.29–2.20 (m, 2H), 2.11 (ddd, J = 13.2, 9.1, 4.5 Hz, 1H), 1.69–1.56 (m, 4H), 1.44–1.28 (m, 8H), 1.06 (s, 9H). ^{13}C NMR (201 MHz, CD_3OD) δ 174.66, 173.08, 172.84, 170.99, 158.76, 157.61, 156.78, 155.55, 152.02, 150.04, 148.37, 139.10, 135.75, 133.68, 128.97, 127.62, 126.47, 124.48, 120.40 (d, J(C, F) = 18.1 Hz, C-F), 116.37 (d, J(C, F) = 24.1 Hz, C-H), 107.34, 103.63, 99.35, 69.68, 66.79, 59.46, 57.59, 56.63, 56.14, 54.75, 51.81, 51.52, 48.47, 47.41, 42.30, 38.31, 37.55, 35.28, 35.19, 32.22, 29.05, 28.96, 28.88, 25.66, 25.60, 24.78, 23.41, 14.27. HPLC 99% pure, t_R =

4.00 min; HRMS *m*/*z* [M + H]$^+$ calculated for $C_{55}H_{72}ClFN_9O_7S^+$ 1056.4942, found 1056.4626.

3-(4-(3-((4-((3-Chloro-4-fluorophenyl)amino)-7-methoxyquinazolin-6-yl)oxy)propyl)piperazin-1-yl)-N-(2-(2-((2-(2,6-dioxopiperidin-3-yl)-1,3-dioxoisoindolin-4-yl)amino)ethoxy)ethyl)-propenamide (7).—Compound **7** was prepared following the general procedure for preparing compound **1** from 3-(4-(3-((4-((3-chloro-4-fluorophenyl)amino)-7-methoxyquinazolin-6-yl)oxy)propyl)-piperazin-1-yl)propanoic acid (**14**, 12.0 mg, 0.02 mmol) and 21 (8.2 mg, 0.02 mmol). Yellow solid (6.4 mg, 37% yield). ^{1}H NMR (600 MHz, CD_3OD) δ 8.73 (s, 1H), 7.96–7.92 (m, 2H), 7.69–7.63 (m, 1H), 7.54 (dd, *J* = 8.6, 7.1 Hz, 1H), 7.37 (t, *J* = 8.9 Hz, 1H), 7.26 (s, 1H), 7.08 (d, *J* = 8.6 Hz, 1H), 7.02 (d, *J* = 7.0 Hz, 1H), 5.05 (dd, *J* = 12.7, 5.5 Hz, 1H), 4.32 (t, *J* = 5.6 Hz, 2H), 4.10–4.04 (m, 4H), 3.72 (t, *J* = 5.1 Hz, 2H), 3.60 (t, *J* = 5.2 Hz, 2H), 3.49 (t, *J* = 5.1 Hz, 2H), 3.46–3.39 (m, 2H), 3.39–3.32 (m, 2H), 3.28–3.07 (m, 8H), 2.85 (ddd, *J* = 17.3, 13.8, 5.3 Hz, 1H), 2.77–2.62 (m, 3H), 2.59 (t, *J* = 6.6 Hz, 2H), 2.35–2.27 (m, 2H), 2.15–2.05 (m, 1H). HPLC 98% pure, t_R = 3.68 min; HRMS *m*/*z* [M + H]$^+$ calculated for $C_{42}H_{47}ClFN_9O_8^+$ 860.3293, found 860.3317.

3-(4-(3-((4-((3-Chloro-4-fluorophenyl)amino)-7-methoxyquina-zolin-6-yl)oxy)propyl)piperazin-1-yl)-N-(17-((2-(2,6-dioxopiperidin-3-yl)-1,3-dioxois oindolin-4-yl)amino)-3,6,9,12,15-pentaoxaheptadecyl)propenamide (8).—Compound **8** was prepared following the general procedure for preparing compound **1** from 3-(4-(3-((4-((3-chloro-4-fluorophenyl)amino)-7-methoxyquinazolin-6-yl)-oxy)propyl)piperazin-1-yl)propanoic acid (14, 12.0 mg, 0.02 mmol) and **22** (11.6 mg, 0.02 mmol). Yellow solid (12.3 mg, 59% yield). ^{1}H NMR (600 MHz, CD_3OD) δ 8.73 (d, *J* = 1.7 Hz, 1H), 7.97–7.90 (m, 2H), 7.66 (ddd, *J* = 9.0, 4.3, 2.4 Hz, 1H), 7.51 (ddd, *J* = 8.7, 7.0, 1.6 Hz, 1H), 7.36 (td, *J* = 8.8, 1.6 Hz, 1H), 7.26 (d, *J* = 1.6 Hz, 1H), 7.04 (dd, *J* = 8.7, 1.6 Hz, 1H), 7.00 (dd, *J* = 7.1, 1.6 Hz, 1H), 5.04 (ddd, *J* = 12.6, 5.5, 1.7 Hz, 1H), 4.34 (t, *J* = 5.6 Hz, 2H), 4.08 (s, 3H), 3.71 (td, *J* = 5.2, 1.6 Hz, 2H), 3.68–3.56 (m, 18H), 3.54 (td, *J* = 5.4, 1.6 Hz, 2H), 3.46 (q, *J* = 8.5, 6.9 Hz, 5H), 3.40–3.32 (m, 7H), 3.25 (t, *J* = 6.8 Hz, 2H), 2.90–2.79 (m, 1H), 2.78–2.59 (m, 4H), 2.41–2.30 (m, 2H), 2.14–2.06 (m, 1H). HPLC 97% pure, t_R = 3.77 min; HRMS *m*/*z* [M + H]$^+$ calculated for $C_{50}H_{63}ClFN_9O^+$ 1036.4269, found 1036.4352.

3-(4-(3-((4-((3-Chloro-4-fluorophenyl)amino)-7-methoxyquinazolin-6-yl)oxy)propyl)piperazin-1-yl)-N-(6-((2-(2,6-dioxopiperidin-3-yl)-1,3-dioxoisoindolin-4-yl)amino)hexyl)propenamide (9).—Compound **9** was prepared following the general procedure for preparing compound **1** from 3-(4-(3-((4-((3-chloro-4-fluorophenyl)amino)-7-methoxyquinazolin-6-yl)oxy)propyl)piperazin-1-yl)propanoic acid (**14**, 12.0 mg, 0.02 mmol) and 23 (9.2 mg, 0.02 mmol). Yellow solid (14.1 mg, 85% yield). ^{1}H NMR (600 MHz, CD_3OD) δ 8.73 (s, 1H), 7.97–7.90 (m, 2H), 7.66 (ddd, J = 8.9, 4.1, 2.6 Hz, 1H), 7.51 (dd, J = 8.6, 7.1 Hz, 1H), 7.36 (t, J = 8.9 Hz, 1H), 7.26 (s, 1H), 7.00 (dd, J = 11.4, 7.8 Hz, 2H), 5.04 (dd, J = 12.8, 5.5 Hz, 1H), 4.35 (t, J = 5.5 Hz, 2H), 4.08 (s, 3H), 3.68–3.43 (m, 10H), 3.41 (t, J = 7.1 Hz, 2H), 3.34 (t, J = 6.7 Hz, 2H), 3.21 (t, J = 7.0 Hz, 2H), 2.84 (ddd, J = 17.6, 14.0, 5.3 Hz, 1H), 2.76–2.63 (m, 4H), 2.42–2.35 (m, 2H), 2.13–

2.05 (m, 1H), 1.71–1.62 (m, 2H), 1.59–1.50 (m, 2H), 1.50–1.38 (m, 4H). HPLC 95% pure, t_R = 3.84 min; HRMS m/z $[M + H]^+$ calculated for $C_{44}H_{52}ClFN_9O_7^+$ 872.3657, found 872.3655.

3-(4-(3-((4-((3-Chloro-4-fluorophenyl)amino)-7-methoxyquinazolin-6-yl)oxy)propyl)piperazin-1-yl)-N-(8-((2-(2,6-dioxopiperidin-3-yl)-1,3-dioxoisoindolin-4-yl)oxy)octyl)propanamide (10).—To the solution of 3-(4-(3-((4-((3-chloro-4-fluorophenyl)amino)-7-methoxyquinazolin-6-yl)oxy)propyl)piperazin-1-yl)propanoic acid (**4**, 10.4 mg, 0.02 mmol) in DMSO (1 mL) were added 4-((8-aminooctyl)-oxy)-2-(2,6-dioxopiperidin-3-yl)isoindoline-1,3-dione (**26**, 8.0 mg, 0.02 mmol, 1.0 equiv), EDCI (6.0 mg, 0.03 mmol, 1.5 equiv), HOAt (4.2 mg, 0.03 mmol, 1.5 equiv), and NMM (6.1 mg, 0.06 mmol, 3.0 equiv). After being stirring overnight at room temperature, the resulting mixture was purified by preparative HPLC (10–100% methanol/0.1% TFA in H_2O) to afford the title compound **10** as white solid in TFA salt form (16.8 mg, 93% yield). ^{1}H NMR (600 MHz, CD_3OD) δ 8.73 (s, 1H), 7.94 (s, 2H), 7.79–7.57 (m, 2H), 7.47–7.30 (m, 3H), 7.26 (s, 1H), 5.09 (dd, J = 12.8, 5.4 Hz, 1H), 4.35 (t, J = 5.5 Hz, 2H), 4.19 (t, J = 6.2 Hz, 2H), 4.08 (s, 3H), 3.61–3.37 (m, 11H), 3.20 (t, J = 7.0 Hz, 2H), 2.91–2.82 (m, 1H), 2.78–2.62 (m, 4H), 2.41–2.35 (m, 2H), 2.21–2.02 (m, 1H), 1.86–1.80 (m, 2H), 1.56–1.48 (m, 4H), 1.44–1.33 (m, 7H). ^{13}C NMR (201 MHz, d-DMSO) δ 173.29, 170.44, 168.83, 167.33, 165.80, 158.59, 156.85, 156.48, 154.84, 149.31(d, J (C, F) = 50.1 Hz, C-F), 137.52, 136.27, 134.73, 133.69, 126.99, 125.77, 120.26, 119.54, 119.44, 117.14 (d, J (C, F) = 23.1 Hz, C-H) 116.65, 115.60, 107.80, 106.00, 100.36, 69.28, 67.63, 57.03, 49.21, 49.05, 48.52, 39.14, 31.43, 29.94, 29.40, 29.11, 28.88, 26.83, 25.73, 23.69, 22.48. HPLC 98% pure, t_R = 4.22 min; HRMS m/z $[M + H]^+$ calculated for $C_{46}H_{55}ClFN_8O_8^+$ 901.3810, found 901.3916.

N-(3-Chloro-4-fluorophenyl)-7-methoxy-6-(3-(piperazin-1-yl)-propoxy)quinazolin-4-amine (13).—To the suspension of commercially available 4-((3-chloro-4-fluorophenyl)amino)-7-methoxyquinazolin-6-ol (**11**, 942 mg, 2.94 mmol) and potassium carbonate (1.2 g, 8.82 mmol, 3.0 equiv) in DMF (20 mL) was added tert-butyl 4-(3-bromopropyl)piperazine-1-carboxylate (**12**, 903 mg, 2.94 mmol, 1.0 equiv). After stirring overnight at 80 °C, water was added, and the mixture was extracted with ethyl acetate (3 × 20 mL), dried over Na_2SO_4, filtered, and concentrated. The crude product was purified by reverse-phase ISCO (10–100% methanol/0.1% TFA in H_2O) to afford white solid in TFA salt form (1.56 g, 97% yield). This product was dissolved in DCM (8 mL) and TFA (8 mL). The resulting mixture was stirred for 30 min. Then, it was concentrated and purified by reverse-phase ISCO (10–100% methanol/0.1% TFA in H_2O) to afford the title compound **3** as white solid in TFA salt form (1.25 g, 98% yield). ^{1}H NMR (600 MHz, CD_3OD) δ 8.74 (s, 1H), 7.98 (s, 1H), 7.66 (dt, J = 9.2, 3.4 Hz, 1H), 7.43–7.31 (m, 1H), 7.27 (d, J = 4.6 Hz, 2H), 4.37 (t, J = 5.6 Hz, 2H), 4.08 (s, 3H), 3.71–3.37 (m, 6H), 3.33–3.21 (m, 4H), 2.39 (t, J = 7.8 Hz, 2H). HPLC 98% pure, t_R = 3.40 min; HRMS m/z $[M + H]^+$ calculated for $C_{22}H_{26}ClFN_5O_2^+$ 446.1754, found 446.1743.

3-(4-(3-((4-((3-Chloro-4-fluorophenyl)amino)-7-methoxyquinazolin-6-yl)oxy)propyl)piperazin-1-yl)propanoic Acid (14).—To the suspension of compound

13 (888 mg, 2 mmol) and potassium carbonate (828 mg, 6 mmol, 3.0 equiv) in DMF (10 mL) was added ethyl 3-bromopropanoate (724 mg, 4 mmol, 2.0 equiv). After being stirring overnight at 80 °C, water was added, and the mixture was extracted with ethyl acetate (3 × 15 mL), dried over Na_2SO_4, filtered, and concentrated. The crude product was purified by reverse-phase ISCO (10–100% methanol/0.1% TFA in H_2O) to afford white solid in TFA salt form (822 mg, 75% yield). This product was dissolved in THF (5 mL) and water (5 mL). After stirring overnight at ambient temperature, it was concentrated and purified by reverse-phase ISCO (10–100% methanol/0.1% TFA in H_2O) to afford the title compound **14** as white solid in TFA salt form (834 mg, 98% yield). ^{1}H NMR (600 MHz, CD_3OD) δ 8.74 (s, 1H), 7.98 (s, 1H), 7.94 (dd, J = 6.6, 2.7 Hz, 1H), 7.72–7.59 (m, 1H), 7.37 (t, J = 8.9 Hz, 1H), 7.27 (s, 1H), 4.35 (t, J = 5.6 Hz, 2H), 4.09 (s, 3H), 3.38–3.32 (m, 4H), 3.27 (t, J = 7.3 Hz, 2H), 3.22–3.16 (m, 4H), 3.13 (t, J = 6.9 Hz, 2H), 2.70 (t, J = 6.9 Hz, 2H), 2.34 (t, J = 6.7 Hz, 2H). HPLC 97% pure, t_R = 3.56 min; HRMS m/z $[M + H]^+$ calculated for $C_{25}H_{30}ClFN_5O_4^+$ 518.1965, found 518.1976.

3-(3-(((S)-1-((2S,4R)-4-Hydroxy-2-((4-(4-methylthiazol-5-yl)-benzyl)carbamoyl) pyrrolidin-1-yl)-3,3-dimethyl-1-oxobutan-2-yl)-amino)-3-oxopropoxy)propanoic Acid (15).—To a solution of 3,3′-oxydipropionic acid (648 mg, 4 mmol) in DMSO (10 mL) were added N-methylmorpholine (NMM, 10 mmol), (2S,4R)-1-((S)-2-amino-3,3-dimethylbutanoyl)-4-hydroxy-N-(4-(4-methylthiazol-5-yl)-benzyl)pyrrolidine-2-carboxamide (VHL-1, 860 mg, 2 mmol), 1-hydroxy-7-azabenzo-triazole (HOAt, 326 mg, 2.4 mmol), and 1-ethyl-3-(3-dimethylaminopropyl)carbodiimide (EDCI, 461 mg, 2.4 mmol) at 0 °C. The resulting reaction solution was stirred at 0 °C for 6 h and then at RT overnight. The progress of the reaction was monitored by LC/MS. After VHL-1 was totally consumed, the reaction was concentrated, and the resulting residue was purified by reverse-phase chromatography to yield the product (450 mg, 63%) as white solid. ^{1}H NMR (600 MHz, CD_3OD) δ 9.00 (s, 1H), 7.45 (d, J = 22.1 Hz, 4H), 4.64 (s, 1H), 4.61–4.44 (m, 3H), 4.36 (d, J = 15.4 Hz, 1H), 3.84 (dd, J = 57.3, 10.5 Hz, 2H), 3.75–3.56 (m, 4H), 2.60–2.39 (m, 7H), 2.24–2.17 (m, 1H), 2.11–2.03 (m, 1H), 1.03 (s, 9H). HRMS (ESI-TOF) m/z: $[M + H]^+$ calculated for $C_{28}H_{39}N_4O_7S$, 575.2534; found: 575.2543.

(S)-15-((2S,4R)-4-Hydroxy-2-((4-(4-methylthiazol-5-yl)benzyl)-carbamoyl) pyrrolidine-1-carbonyl)-16,16-dimethyl-13-oxo-4,7,10-trioxa-14-azaheptadecanoic Acid (16).—(677 mg, 57%) as white solid. ^{1}H NMR (600 MHz, CD_3OD) δ 8.95 (s, 1H), 7.47 (d, J = 8.1 Hz, 2H), 7.42 (d, J = 8.1 Hz, 2H), 4.65 (s, 1H), 4.59–4.51 (m, 2H), 4.49 (s, 1H), 4.35 (d, J = 15.5 Hz, 1H), 3.89 (d, J = 11.1 Hz, 1H), 3.80 (dd, J = 10.9, 3.9 Hz, 1H), 3.76–3.67 (m, 4H), 3.66–3.54 (m, 8H), 2.60–2.50 (m, 3H), 2.50–2.43 (m, 4H), 2.21 (dd, J = 13.1, 7.6 Hz, 1H), 2.08 (ddd, J = 13.3, 9.1, 4.5 Hz, 1H), 1.04 (s, 9H). HRMS (ESI-TOF) m/z: $[M + H]^+$ calculated for $C_{32}H_{47}N_4O_9S$, 663.3058; found: 663.3059.

(S)-19-((2S,4R)-4-Hydroxy-2-((4-(4-methylthiazol-5-yl)benzyl)-carbamoyl) pyrrolidine-1-carbonyl)-20,20-dimethyl-17-oxo-3,6,9,12,15-pentaoxa-18-azahenicosanoic Acid (17).—(496 mg, 54%) as white solid. ^{1}H NMR (600 MHz, CD_3OD) δ 8.89 (s, 1H), 7.47 (d, J = 8.1 Hz, 2H), 7.42 (d, J = 8.1 Hz, 2H), 4.69 (s, 1H),

4.59–4.46 (m, 3H), 4.36 (d, J = 15.5 Hz, 1H), 4.16–4.00 (m, 4H), 3.87 (d, J = 11.0 Hz, 1H), 3.80 (dd, J = 11.0, 3.7 Hz, 1H), 3.76–3.53 (m, 16H), 2.48 (s, 3H), 2.22 (dd, J = 13.1, 7.6 Hz, 1H), 2.08 (ddd, J = 13.3, 9.2, 4.4 Hz, 1H), 1.04 (s, 7H). HRMS (ESI-TOF) m/z: $[M + H]^+$ calculated for $C_{34}H_{51}N_4O_{11}S$, 723.3270; found: 723.3269.

4-(((S)-1-((2S,4R)-4-Hydroxy-2-((4-(4-methylthiazol-5-yl)benzyl)-carbamoyl) pyrrolidin-1-yl)-3,3-dimethyl-1-oxobutan-2-yl)amino)-4-oxobutanoic Acid (18).—(810 mg, 85%) as white solid. ^{1}H NMR (600 MHz CD_3OD) δ 9.10 (s, 1H), 7.51 (d, J = 7.8 Hz, 2H), 7.44 (d, J = 8.4 Hz, 2H), 4.64 (s, 1H), 4.60–4.49 (m, 3H), 4.39 (d, J = 15.6 Hz, 1H), 3.91 (d, J = 10.8 Hz, 1H), 3.82 (dd, J = 9.6, 3.6 Hz, 1H), 2.67–2.55 (m, 4H), 2.52 (s, 3H), 2.25–2.22 (m, 1H), 2.12–2.07 (m, 1H), 1.06 (s, 9H). HRMS (ESI-TOF) m/z: $[M + H]^+$ calculated for $C_{26}H_{35}N_4O_6S$, 531.2272, found 531.2280.

7-(((S)-1-((2S,4R)-4-Hydroxy-2-((4-(4-methylthiazol-5-yl)benzyl)-carbamoyl) pyrrolidin-1-yl)-3,3-dimethyl-1-oxobutan-2-yl)amino)-7-oxoheptanoic Acid (19).—(810 mg, 79%) as white solid. ^{1}H NMR (600 MHz CD_3OD) δ 8.98 (s, 1H), 7.50 (d, J = 8.4 Hz, 2H), 7.44 (d, J = 9.0 Hz, 2H), 4.65 (s, 1H), 4.60–4.49 (m, 3H), 4.38 (d, J = 15.6 Hz, 1H), 3.93 (d, J = 10.8 Hz, 1H), 3.82 (dd, J = 11.4, 3.6 Hz, 1H), 2.51 (s, 3H), 2.35–2.22 (m, 5H), 2.13–2.08 (m, 1H), 1.68–1.59 (m, 4H),1.42–1.34 (m, 2H), 1.06 (s, 9H). HRMS (ESI-TOF) m/z: $[M + H]^+$ calculated for $C_{29}H_{41}N_4O_6S$, 573.2741, found 573.2754.

11-(((S)-1-((2S,4R)-4-Hydroxy-2-((4-(4-methylthiazol-5-yl)-benzyl)carbamoyl)pyrrolidin-1-yl)-3,3-dimethyl-1-oxobutan-2-yl)-amino)-11-oxoundecanoic Acid (20).—(574 mg, 76% yield) as white solid. ^{1}H NMR (600 MHz, CD_3OD) δ 8.99 (d, J = 5.3 Hz, 1H), 7.47 (dd, J = 8.2, 2.2 Hz, 2H), 7.42 (dd, J = 8.3, 2.9 Hz, 2H), 4.65–4.61 (m, 1H), 4.59–4.46 (m, 3H), 4.35 (d, J = 15.5 Hz, 1H), 3.93–3.86 (m, 1H), 3.80 (dt, J = 11.0, 3.5 Hz, 1H), 2.48 (s, 3H), 2.36–2.16 (m, 4H), 2.08 (ddd, J = 13.3, 9.1, 4.5 Hz, 1H), 1.65–1.52 (m, 4H), 1.39–1.22 (m, 11H), 1.03 (s, 9H). HPLC 95% pure, t_R = 4.25 min; HRMS m/z $[M + H]^+$ calculated for $C_{33}H_{49}N_4O_6S^+$ 629.3367, found 629.3343.

4-((8-Aminooctyl)oxy)-2-(2,6-dioxopiperidin-3-yl)isoindoline-1,3-dione (26).—To the suspension of 2-(2,6-dioxopiperidin-3-yl)-4-hydroxyisoindoline-1,3-dione (24, 55.0 mg, 0.2 mmol), sodium bicarbonate (1.2 g, 0.46 mmol, 2.3 equiv), and sodium iodide (6 mg, 0.04 mmol, 0.2 equiv) in DMF (2 mL) was added tert-butyl (8-iodooctyl)carbamate, which was prepared according to the previously reported procedures[46] (25, 85.2 mg, 0.24 mmol, 1.2 equiv). After stirring at 65 °C for 2 days, the reaction mixture was purified by preparative HPLC to yield white solid (46.8 mg, 47%). MS (ESI) m/z 502.5 $[M + H]^+$. This white solid was dissolved in DCM (1 mL) and TFA (1 mL). The resulting mixture was stirred for 30 min. Then, it was concentrated and purified by preparative HPLC (10–100% acetonitrile/0.1% TFA in H_2O) to yield title compound **26** as white solid (28.2 mg, 76%). ^{1}H NMR (600 MHz, CD_3OD) δ 7.75 (t, J = 7.9 Hz, 1H), 7.41 (dd, J = 8.3, 3.8 Hz, 2H), 5.09 (dd, J = 12.9, 5.4 Hz, 1H), 4.21 (t, J = 6.4 Hz, 2H), 2.96–2.79 (m, 3H), 2.79–2.61 (m, 2H), 2.12 (dd, J = 12.6, 5.9 Hz, 1H), 1.85 (p, J = 6.7 Hz, 2H), 1.65 (p, J = 7.3 Hz, 2H), 1.54 (q, J = 7.4 Hz, 2H), 1.47–1.30 (m, 6H). HPLC 95% pure, t_R = 4.19 min; HRMS m/z $[M + H]^+$ calculated for $C_{21}H_{28}N_3O_5^+$ 402.2023, found 402.2046.

(2R,4S)-1-((S)-2-(11-(4-(3-((4-((3-Chloro-4-fluorophenyl)amino)-7-methoxyquinazolin-6-yl)oxy)propyl)piperazin-1-yl)-11-oxoundecanamido)-3,3-dimethylbutanoyl)-4-hydroxy-N-(4-(4-methylthiazol-5-yl)benzyl)pyrrolidine-2-carboxamide (27).—Compound **27** was prepared following the general procedure for preparing compound **1** from N-(3-chloro-4-fluorophenyl)-7-methoxy-6-(3-(piperazin-1-yl)-propoxy)quinazolin-4-amine (**13**, 11.0 mg, 0.02 mmol) and 11-(((S)-1-((2R,4S)-4-hydroxy-2-((4-(4-methylthiazol-5-yl)benzyl)-carbamoyl)pyrrolidin-1-yl)-3,3-dimethyl-1-oxobutan-2-yl)amino)-11-oxoundecanoic acid (**31**, 13.6 mg, 0.02 mmol). White solid (18.4 mg, 87% yield). ^{1}H NMR (600 MHz, CD_3OD) δ 9.00 (s, 1H), 8.74 (s, 1H), 8.06–7.86 (m, 2H), 7.74–7.59 (m, 1H), 7.54–7.08 (m, 6H), 4.58 (dd, J = 8.4, 6.5 Hz, 1H), 4.54–4.46 (m, 2H), 4.43 (s, 1H), 4.41–4.30 (m, 3H), 4.08 (s, 3H), 3.99 (dd, J = 10.8, 4.9 Hz, 1H), 3.93–3.35 (m, 6H), 3.19 (d, J = 1.5 Hz, 5H), 2.50 (s, 3H), 2.43 (dd, J = 9.1, 6.2 Hz, 4H), 2.31–2.09 (m, 3H), 2.02 (ddd, J = 14.6, 9.0, 6.0 Hz, 1H), 1.57 (p, J = 7.5 Hz, 2H), 1.50–1.12 (m, 12H), 1.07 (s, 9H). ^{13}C NMR (201 MHz, CD_3OD) δ 175.56, 173.11, 172.78, 171.19, 158.78, 157.58, 156.79, 155.56, 151.48, 150.02, 148.47, 147.51, 138.87, 135.92, 133.70, 132.13, 129.99, 128.97, 127.29, 126.49, 124.50 (d, J (C, F) = 16.0 Hz), 116.49 (d, J (C, F) = 22.1 Hz, C-F), 107.36, 103.60, 99.43, 69.12, 66.79, 59.58, 58.69, 56.11, 55.42, 54.77, 51.82, 51.52, 42.26, 42.10, 38.31, 37.71, 34.90, 33.95, 32.21, 29.07, 28.96, 25.66, 25.38, 24.77, 23.43, 14.55. HPLC 98% pure, t_R = 4.14 min; HRMS m/z $[M + H]^+$ calculated for $C_{55}H_{72}ClFN_9O_7S^+$ 1056.4942, found 1056.4910.

3-(4-(3-((4-((3-Chloro-4-fluorophenyl)amino)-7-methoxyquina-zolin-6-yl)oxy)propyl)piperazin-1-yl)-N-(8-((2-(1-methyl-2,6-dioxopiperidin-3-yl)-1,3-dioxoisoindolin-4-yl)oxy)octyl)propanamide (28).—Compound **28** was prepared following the general procedure for preparing compound **10** from 3-(4-(3-((4-((3-chloro-4-fluorophenyl)amino)-7-methoxyquinazolin-6-yl)oxy)propyl)-piperazin-1-yl)propanoic acid (**14**, 13.4 mg, 0.025 mmol) and 4-((8-aminooctyl)oxy)-2-(1-methyl-2,6-dioxopiperidin-3-yl)isoindoline-1,3-dione (33, 10.8 mg, 0.025 mmol). White solid (13.8 mg, yield 60%). ^{1}H NMR (600 MHz, CD_3OD) δ 8.74 (d, J = 1.2 Hz, 1H), 7.98–7.89 (m, 2H), 7.76–7.69 (m, 1H), 7.66 (ddd, J = 8.9, 4.1, 2.6 Hz, 1H), 7.43–7.32 (m, 3H), 7.27 (s, 1H), 5.12 (dd, J = 12.9, 5.4 Hz, 1H), 4.37 (t, J = 5.5 Hz, 2H), 4.19 (t, J = 6.3 Hz, 2H), 4.09 (s, 3H), 3.77–3.62 (m, 7H), 3.48 (dt, J = 21.2, 6.9 Hz, 4H), 3.19 (t, J = 7.2 Hz, 2H), 3.14 (s, 3H), 2.76–2.62 (m, 5H), 2.42 (p, J = 6.7 Hz, 2H), 2.13–2.05 (m, 1H), 1.88–1.77 (m, 2H), 1.52 (q, J = 7.0 Hz, 4H), 1.44–1.31 (m, 7H). ^{13}C NMR (201 MHz, CD_3OD) δ 172.24, 170.87, 170.04, 167.24, 165.95, 158.67, 157.59, 156.76, 156.61, 155.52, 150.12, 148.32, 136.55, 135.68, 133.61, 126.42, 124.47, 120.38 (d, J (C, F) = 20.1 Hz), 119.14, 116.62, 116.37 (d, J (C, F) = 22.1 Hz), 114.88, 107.31, 103.46, 99.32, 69.13, 66.90, 56.15, 54.48, 52.81, 50.09, 49.66, 49.55, 39.13, 31.07, 30.47, 28.88, 28.84, 28.57, 26.48, 26.00, 25.46, 23.92, 21.51. HPLC 98% pure, t_R = 4.32 min; HRMS m/z $[M + H]^+$ calculated for $C_{47}H_{57}ClFN\ O^+$ 915.3966, found 915.3967.

11-(((S)-1-((2R,4S)-4-Hydroxy-2-((4-(4-methylthiazol-5-yl)-benzyl)carbamoyl)pyrrolidin-1-yl)-3,3-dimethyl-1-oxobutan-2-yl)-amino)-11-oxoundecanoic Acid (31).—Compound **31** was prepared following the general procedure for preparing compound **15** from (2R,4S)-1-((S)-2-amino-3,3-

dimethylbutanoyl)-4-hydroxy-N-(4-(4-methylthiazol-5-yl)benzyl)pyrrolidine-2-carboxamide (**29**, 108 mg, 0.25 mmol) and undecanedioic acid (30, 65 mg, 0.3 mmol, 1.2 equiv). White solid (67.2 mg, 43% yield). ^{1}H NMR (600 MHz, CD_3OD) δ 8.99 (s, 1H), 7.46–7.42 (m, 2H), 7.39 (d, J = 8.2 Hz, 2H), 4.59 (dd, J = 8.4, 6.5 Hz, 1H), 4.53 (d, J = 15.7 Hz, 1H), 4.51–4.46 (m, 1H), 4.43 (s, 1H), 4.34 (d, J = 15.7 Hz, 1H), 3.99 (dt, J = 12.1, 6.0 Hz, 1H), 3.72 (ddd, J = 11.0, 3.7, 1.1 Hz, 1H), 2.50 (s, 3H), 2.30–2.12 (m, 5H), 2.00 (ddd, J = 14.6, 8.9, 6.0 Hz, 1H), 1.54 (p, J = 7.4 Hz, 2H), 1.48–1.39 (m, 1H), 1.38–1.13 (m, 11H), 1.07 (s, 9H). HPLC 97% pure, t_R = 4.30 min; HRMS m/z $[M + H]^+$ calculated for $C_{33}H_{49}N_4O_6S^+$ 629.3367, found 629.3378.

4-((8-Aminooctyl)oxy)-2-(1-methyl-2,6-dioxopiperidin-3-yl)-isoindoline-1,3-dione (33).—To the suspension of tert-butyl (8-((2-(2,6-dioxopiperidin-3-yl)-1,3-dioxoisoindolin-4-yl)oxy)octyl)-carbamate (265 mg, 0.53 mmol) and potassium carbonate (110 mg, 0.8 mmol, 1.5 equiv) in DMF (5 mL) was added iodomethane (114 mg, 0.8 mmol, 1.5 equiv). After stirring overnight at room temperature for 4 h, water was added, and the mixture was extracted with ethyl acetate (3 × 15 mL), dried over Na_2SO_4, filtered, and concentrated. The crude product was dissolved in DCM (3 mL) and TFA (3 mL). The resulting mixture was stirred for 30 min. Then, it was concentrated and purified by reverse-phase ISCO (10–100% methanol/0.1% TFA in H_2O) to afford the title compound **33** as white solid in TFA salt form (179 mg, 81% yield). ^{1}H NMR (600 MHz, CD_3OD) δ 7.76 (ddd, J = 8.5, 7.2, 1.0 Hz, 1H), 7.43 (dd, J = 7.9, 4.7 Hz, 2H), 5.16–5.05 (m, 1H), 4.22 (t, J = 6.3 Hz, 2H), 3.15 (s, 3H), 2.89 (ddd, J = 12.8, 7.8, 5.2 Hz, 4H), 2.68 (qd, J = 12.6, 6.1 Hz, 1H), 2.14–2.05 (m, 1H), 1.90–1.81 (m, 2H), 1.69–1.61 (m, 2H), 1.59–1.52 (m, 2H), 1.48–1.35 (m, 6H). HPLC 98% pure, t_R = 4.28 min; HRMS m/z $[M + H]^+$ calculated for $C_{22}H_{30}N_3O_5^+$ 416.2180, found 416.2167.

EGFR Binding Assay.

Binding affinities of gefitinib, compounds **6**, **10**, **27**, and **28** to EGFR WT and EGFR L858R were determined by DiscoverX using the KINOMEscan assay, a competition binding assay that quantitatively measures the ability of a compound to compete with an immobilized, active-site-directed ligand. The assay was performed by combining three components: DNA-tagged EGFR, immobilized ligand, and a test compound. The ability of the test compound to compete with the immobilized ligand was measured by quantitative PCR of the DNA tag. The K_d values were determined using an 11-point 3-fold compound dilution (the top concentration of 1 μM for gefitinib and 30 μM for other compounds) with three DMSO control points in duplicates.

Cell Culture.

HCC-827 cells and H3255 cells were purchased from ATCC. Both cell lines were cultured in RPMI/1640 medium supplemented with 20% FBS (HCC-827 cells)/20% FBS (H3255 cells) and 50 μg/mL penicillin/streptomycin. Cells were cultured in an incubator at 37 °C with 5% CO_2.

Western Blot Analysis.

Cultured cells were washed with PBS twice and then lysed in a 1X Laemmli sample buffer (BIO-RAD) directly. Lysates were heated at 100 °C for 10 min and centrifuged at 14 000 rpm for 10 min before loading to the 4–15% precast gels (BIO-RAD). Samples were running under 80 V for 15 min, then switched to 150 V for another 1 h, and then transferred to PVDF membranes at 100 V, 90 min. Membranes were then blocked in a 5% skim milk TBST buffer for 1 h at room temperature, followed by primary antibody incubation overnight at 4 °C. HRP-conjugated secondary antibody was then applied and incubated for 2 h at room temperature. Membranes were imaged by a ChemiDoc MP Imaging system (BIO-RAD) and organized with Image Lab software.

Cell Proliferation Assay.

2000/well HCC-827 cells or 4000/well H3255 cells were planted to 96 wells a night before and then treated with indicated doses of EGFR degraders or controls for another 3 days. Cell proliferation/survival was measured using Cell Counting Kit-8 (Sigma-Aldrich) following the manufacturer's instruction and plotted via Graphpad 6.

Liquid Chromatography–Mass Spectrometry (LC–MS).

The clean peptides were dissolved in 0.1% formic acid and analyzed on a Q-Exactive HF-X coupled with an Easy nanoLC 1200 (Thermo Fisher Scientific, San Jose, CA). Peptides of 1 mg were loaded onto an Acclain PepMap RSLC C18 column (250 mm × 75 μm ID, C18, 2 μm, Thermo Fisher). Analytical separation of all peptides was achieved with a 100 min or 140 min gradient. A linear gradient of 5–30% buffer B over 75 min or 100 min was executed at a 300 nL/min flow rate following a ramp to 100% B in 1 or 5, and 9 min or 15 min wash with 100% B, where buffer A was aqueous 0.1% formic acid and buffer B was 80% acetonitrile and 0.1% formic acid.

LC–MS experiments were also performed in a data-dependent mode with full MS (externally calibrated to a mass accuracy of <5 ppm and a resolution of 60 000 at m/z 200) followed by high-energy collision-activated dissociation-MS/MS of the top 20 most intense ions with a resolution of 15 000 at m/z 200. High-energy collision-activated dissociation-MS/MS was used to dissociate peptides at a normalized collision energy of 27 eV in the presence of nitrogen bath gas atoms. Dynamic exclusion was 30.0 s. There were three biological replicates for one treatment, and each sample was subjected to two technical LC–MS replicates.

Raw data processing and analysis. Mass spectra were processed, and peptide identification was performed using the Andromeda search engine found in MaxQuant software version 1.6.0.16 (Max Planck Institute, Germany). All protein database searches were performed against the UniProt human protein sequence database (UP000005640). Peptides were identified with a target-decoy approach using a combined database consisting of reverse protein sequences of the UniProt human. A false discovery rate for both peptide-spectrum match and protein assignment was set at 1%. Search parameters included up to two missed cleavages at Lys/Arg on the sequence, oxidation of methionine, and protein N-terminal acetylation as a dynamic modification. Carbamidomethylation of cysteine residues was

considered as a static modification. Peptide identifications are reported by the filtering of reverse and contaminant entries and assigning to their leading razor protein. LFQ was performed based on peak area. The measured area under the curve of m/z and the retention time-aligned extracted ion chromatogram of a peptide were performed via the label-free quantitation module found in MaxQuant version 1.6.0.16. Data processing and statistical analysis were performed on Perseus (Version 1.6.0.7). Protein quantitation was performed on technical replicates, and a two-sample t-test statistics was used with a p-value of 5% to report statistically significant protein abundance fold changes.

Statistical Analysis.

Data was analyzed using GraphPad 6.0. Half-life ($t_{1/2}$) (time needed for degrading a half of the protein), DC_{50} (concentration that resulted in a 50% EGFR degradation), and IC_{50} (concentration that led to 50% of cell growth inhibition) were calculated using the nonlinear regression-"log (inhibitor) vs response-variable slope" analytical protocol.

Mouse Pharmacokinetic Study.

Compounds **6** and **10** were dissolved in 5% DMA, 25% Solutol HS-15, and 70% normal saline as formulation. Six male Swiss Albino mice were administered intraperitoneally with a solution formulation of each compound at a dose of 50 mg/kg. Plasma samples (approximately 60 μL) were collected from three mice at 0.5, 2, 8, 12, 16, and 24 h. Compound concentrations in plasma at each time point are the average values from three test mice. Error bars represent ± SEM. Experiments involving mice were performed according to the Institutional Animal Care and Use Committee-approved protocol.

Supplementary Material

Refer to Web version on PubMed Central for supplementary material.

ACKNOWLEDGMENTS

J.J. acknowledges the support by an endowed professorship by the Icahn School of Medicine at Mount Sinai.

ABBREVIATIONS USED

EGFR	epidermal growth factor receptor
NSCLC	non-small-cell lung cancers
PROTACs	proteolysis targeting chimeras
TKI	tyrosine kinase inhibitor
PEG	poly(ethylene glycol)
ATP	adenosine triphosphate
EGFR e19d	EGFR mutant with exo 19 deletion
EGFR L858R	EGFR L858R single point mutant

RTK	receptor tyrosine kinase
WT	wild type
VHL	von Hippel–Lindau
CRBN	cereblon
PK	pharmacokinetic
TFA	trifluoroacetic acid
EDCI	1-ethyl-3-(3-dimethylaminopropyl)carbodiimide
HOAt	1-hydroxy-7-azabenzo-triazole
NMM	*N*-methylmorpholine

REFERENCES

(1). Sharma SV; Bell DW; Settleman J; Haber DA Epidermal growth factor receptor mutations in lung cancer. Nat. Rev. Cancer 2007, 7, 169–181. [PubMed: 17318210]

(2). Wieduwilt MJ; Moasser MM The epidermal growth factor receptor family: biology driving targeted therapeutics. Cell Mol. Life Sci 2008, 65, 1566–1584. [PubMed: 18259690]

(3). Seshacharyulu P; Ponnusamy MP; Haridas D; Jain M; Ganti AK; Batra SK Targeting the EGFR signaling pathway in cancer therapy. Expert Opin. Ther. Targets 2012, 16, 15–31. [PubMed: 22239438]

(4). Krause DS; Van Etten RA Tyrosine kinases as targets for cancer therapy. N. Engl. J. Med 2005, 353, 172–187. [PubMed: 16014887]

(5). Nadeem Abbas M; Kausar S; Wang F; Zhao Y; Cui H Advances in targeting the epidermal growth factor receptor pathway by synthetic products and its regulation by epigenetic modulators as a therapy for glioblastoma. Cells 2019, 8, 350–361.

(6). Nicholson RI; Gee JMW; Harper ME EGFR and cancer prognosis. Eur. J. Cancer 2001, 37, 9–15. [PubMed: 11165124]

(7). Hirsch FR; Scagliotti GV; Mulshine JL; Kwon R; Curran WJ; Wu Y-L; Paz-Ares L Lung cancer: current therapies and new targeted treatments. Lancet 2017, 389, 299–311. [PubMed: 27574741]

(8). Herbst RS; Fukuoka M; Baselga J Gefitinib–a novel targeted approach to treating cancer. Nat. Rev. Cancer 2004, 4, 956–965. [PubMed: 15573117]

(9). Cappuzzo F; Ciuleanu T; Stelmakh L; Cicenas S; Szcześna A; Juhaśz E; Esteban E; Molinier O; Brugger W; Melezínek I; Klingelschmitt G; Klughammer B; Giaccone G Erlotinib as maintenance treatment in advanced non-small-cell lung cancer: a multicentre, randomised, placebo-controlled phase 3 study. Lancet Oncol 2010, 11, 521–529. [PubMed: 20493771]

(10). Yun CH; Mengwasser KE; Toms AV; Woo MS; Greulich H; Wong KK; Meyerson M; Eck MJ The T790M mutation in EGFR kinase causes drug resistance by increasing the affinity for ATP. Proc. Natl. Acad. Sci. U.S.A 2008, 105, 2070–2075. [PubMed: 18227510]

(11). Godin-Heymann N; Ulkus L; Brannigan BW; McDermott U; Lamb J; Maheswaran S; Settleman J; Haber DA The T790M "gatekeeper" mutation in EGFR mediates resistance to low concentrations of an irreversible EGFR inhibitor. Mol. Cancer Ther 2008, 7, 874–879. [PubMed: 18413800]

(12). Pao W; Miller VA; Politi KA; Riely GJ; Somwar R; Zakowski MF; Kris MG; Varmus H Acquired resistance of lung adenocarcinomas to gefitinib or erlotinib is associated with a second mutation in the EGFR kinase domain. PLoS Med 2005, 2, No. e73.

(13). Kobayashi S; Boggon TJ; Dayaram T; Janne PA; Kocher O; Meyerson M; Johnson BE; Eck MJ; Tenen DG; Halmos B EGFR mutation and resistance of non-small-cell lung cancer to gefitinib. N. Engl. J. Med 2005, 352, 786–792. [PubMed: 15728811]

(14). Thress KS; Paweletz CP; Felip E; Cho BC; Stetson D; Dougherty B; Lai Z; Markovets A; Vivancos A; Kuang Y; Ercan D; Matthews SE; Cantarini M; Barrett JC; Janne PA; Oxnard GR Acquired EGFR C797S mutation mediates resistance to AZD9291 in non-small cell lung cancer harboring EGFR T790M. Nat. Med 2015, 21, 560–562. [PubMed: 25939061]

(15). Lu X; Yu L; Zhang Z; Ren X; Smaill JB; Ding K Targeting EGFR(L858R/T790M) and EGFR(L858R/T790M/C797S) resistance mutations in NSCLC: Current developments in medicinal chemistry. Med. Res. Rev 2018, 38, 1550–1581. [PubMed: 29377179]

(16). Patel H; Pawara R; Ansari A; Surana S Recent updates on third generation EGFR inhibitors and emergence of fourth generation EGFR inhibitors to combat C797S resistance. Eur. J. Med. Chem 2017, 142, 32–47. [PubMed: 28526474]

(17). Tan CS; Cho BC; Soo RA Next-generation epidermal growth factor receptor tyrosine kinase inhibitors in epidermal growth factor receptor-mutant non-small cell lung cancer. Lung Cancer 2016, 93, 59–68. [PubMed: 26898616]

(18). Wang S; Song Y; Liu D EAI045: The fourth-generation EGFR inhibitor overcoming T790M and C797S resistance. Cancer Lett 2017, 385, 51–54. [PubMed: 27840244]

(19). Li Q; Zhang T; Li S; Tong L; Li J; Su Z; Feng F; Sun D; Tong Y; Wang X; Zhao Z; Zhu L; Ding J; Li H; Xie H; Xu Y Discovery of potent and noncovalent reversible EGFR kinase inhibitors of EGFR(L858R/T790M/C797S). ACS Med. Chem. Lett 2019, 10, 869–873. [PubMed: 31223440]

(20). Park H; Jung H-Y; Mah S; Hong S Discovery of EGF receptor inhibitors that are selective for the d746–750/T790M/C797S mutant through structure-based de novo design. Angew. Chem 2017, 129, 7742–7746.

(21). Shen J; Zhang T; Zhu SJ; Sun M; Tong L; Lai M; Zhang R; Xu W; Wu R; Ding J; Yun CH; Xie H; Lu X; Ding K Structure-based design of 5-methylpyrimidopyridone derivatives as new wild-type sparing inhibitors of the epidermal growth factor receptor triple mutant (EGFR(L858R/T790M/C797S)). J. Med. Chem 2019, 62, 7302–7308. [PubMed: 31298540]

(22). Grabe T; Lategahn J; Rauh D C797S Resistance: The undruggable EGFR mutation in non-small cell lung cancer? ACS Med. Chem. Lett 2018, 9, 779–782. [PubMed: 30128066]

(23). Lai AC; Crews CM Induced protein degradation: an emerging drug discovery paradigm. Nat. Rev. Drug Discovery 2017, 16, 101–114. [PubMed: 27885283]

(24). Toure M; Crews CM Small-molecule PROTACS: new approaches to protein degradation. Angew. Chem., Int. Ed 2016, 55, 1966–1973.

(25). Burslem GM; Crews CM Small-molecule modulation of protein homeostasis. Chem. Rev 2017, 117, 11269–11301. [PubMed: 28777566]

(26). Sakamoto KM; Kim KB; Kumagai A; Mercurio F; Crews CM; Deshaies RJ Protacs: chimeric molecules that target proteins to the Skp1-Cullin-F box complex for ubiquitination and degradation. Proc. Natl. Acad. Sci. U.S.A 2001, 98, 8554–8559. [PubMed: 11438690]

(27). Salami J; Crews CM Waste disposal-An attractive strategy for cancer therapy. Science 2017, 355, 1163–1167. [PubMed: 28302825]

(28). Winter GE; Buckley DL; Paulk J; Roberts JM; Souza A; Dhe-Paganon S; Bradner JE DRUG DEVELOPMENT. Phthalimide conjugation as a strategy for in vivo target protein degradation. Science 2015, 348, 1376–1381. [PubMed: 25999370]

(29). Bondeson DP; Mares A; Smith IE; Ko E; Campos S; Miah AH; Mulholland KE; Routly N; Buckley DL; Gustafson JL; Zinn N; Grandi P; Shimamura S; Bergamini G; Faelth-Savitski M; Bantscheff M; Cox C; Gordon DA; Willard RR; Flanagan JJ; Casillas LN; Votta BJ; den Besten W; Famm K; Kruidenier L; Carter PS; Harling JD; Churcher I; Crews CM Catalytic in vivo protein knockdown by small-molecule PROTACs. Nat. Chem. Biol 2015, 11, 611–617. [PubMed: 26075522]

(30). Noble ME; Endicott JA; Johnson LN Protein kinase inhibitors: insights into drug design from structure. Science 2004, 303, 1800–1805. [PubMed: 15031492]

(31). Bondeson DP; Smith BE; Burslem GM; Buhimschi AD; Hines J; Jaime-Figueroa S; Wang J; Hamman BD; Ishchenko A; Crews CM Lessons in PROTAC design from selective degradation with a promiscuous warhead. Cell Chem. Biol 2018, 25, 78–87. [PubMed: 29129718]

(32). Ottis P; Crews CM Proteolysis-targeting chimeras: induced protein degradation as a therapeutic strategy. ACS Chem. Biol 2017, 12, 892–898. [PubMed: 28263557]

(33). Cromm PM; Crews CM Targeted protein degradation: from chemical biology to drug discovery. Cell Chem. Biol 2017, 24, 1181–1190. [PubMed: 28648379]

(34). Ferguson FM; Gray NS Kinase inhibitors: the road ahead. Nat. Rev. Drug Discovery 2018, 17, 353–377. [PubMed: 29545548]

(35). Pettersson M; Crews CM PROteolysis TArgeting Chimeras (PROTACs)-past, present and future. Drug Discovery Today Technol 2019, 31, 15–27.

(36). Olson CM; Jiang B; Erb MA; Liang Y; Doctor ZM; Zhang Z; Zhang T; Kwiatkowski N; Boukhali M; Green JL; Haas W; Nomanbhoy T; Fischer ES; Young RA; Bradner JE; Winter GE; Gray NS Pharmacological perturbation of CDK9 using selective CDK9 inhibition or degradation. Nat. Chem. Biol 2018, 14, 163–170. [PubMed: 29251720]

(37). Zhao B; Burgess K PROTACs suppression of CDK4/6, crucial kinases for cell cycle regulation in cancer. Chem. Commun 2019, 55, 2704–2707.

(38). Jiang B; Wang ES; Donovan KA; Liang Y; Fischer ES; Zhang T; Gray NS Development of dual and selective degraders of cyclin-dependent kinases 4 and 6. Angew. Chem., Int. Ed 2019, 58, 6321–6326.

(39). Brand M; Jiang B; Bauer S; Donovan KA; Liang Y; Wang ES; Nowak RP; Yuan JC; Zhang T; Kwiatkowski N; Muller AC; Fischer ES; Gray NS; Winter GE Homolog-selective degradation as a strategy to probe the function of CDK6 in AML. Cell Chem. Biol 2019, 26, 300–306 e9. [PubMed: 30595531]

(40). Cromm PM; Samarasinghe KTG; Hines J; Crews CM Addressing kinase-independent functions of Fak via PROTAC-mediated degradation. J. Am. Chem. Soc 2018, 140, 17019–17026. [PubMed: 30444612]

(41). Burslem GM; Smith BE; Lai AC; Jaime-Figueroa S; McQuaid DC; Bondeson DP; Toure M; Dong H; Qian Y; Wang J; Crew AP; Hines J; Crews CM The advantages of targeted protein degradation over inhibition: An RTK case study. Cell Chem. Biol 2018, 25, 67–77. [PubMed: 29129716]

(42). Paez JG; Janne PA; Lee JC; Tracy S; Greulich H; Gabriel S; Herman P; Kaye FJ; Lindeman N; Boggon TJ; Naoki K; Sasaki H; Fujii Y; Eck MJ; Sellers WR; Johnson BE; Meyerson M EGFR mutations in lung cancer: correlation with clinical response to gefitinib therapy. Science 2004, 304, 1497–500. [PubMed: 15118125]

(43). Tahirovic YA; Truax VM; Wilson RJ; Jecs E; Nguyen HH; Miller EJ; Kim MB; Kuo KM; Wang T; Sum CS; Cvijic ME; Schroeder GM; Wilson LJ; Liotta DC Discovery of N-alkyl piperazine side chain based CXCR4 antagonists with improved drug-like properties. ACS Med. Chem. Lett 2018, 9, 446–451. [PubMed: 29795757]

(44). Zhang C; Han XR; Yang X; Jiang B; Liu J; Xiong Y; Jin J Proteolysis targeting chimeras (PROTACs) of anaplastic lymphoma linase (ALK). Eur. J. Med. Chem 2018, 151, 304–314. [PubMed: 29627725]

(45). Li Y; Yang J; Aguilar A; McEachern D; Przybranowski S; Liu L; Yang CY; Wang M; Han X; Wang S Discovery of MD-224 as a first-in-class, highly potent, and efficacious proteolysis targeting chimera Murine Double Minute 2 degrader capable of achieving complete and durable tumor regression. J. Med. Chem 2019, 62, 448–466. [PubMed: 30525597]

(46). Schramm S; Agnetta L; Bermudez M; Gerwe H; Irmen M; Holze J; Littmann T; Wolber G; Trankle C; Decker M Novel BQCA- and TBPB-derived M1 receptor hybrid ligands: orthosteric carbachol differentially regulates partial agonism. Chem-MedChem 2019, 14, 1349–1358.

(47). Buckley DL; Van Molle I; Gareiss PC; Tae HS; Michel J; Noblin DJ; Jorgensen WL; Ciulli A; Crews CM Targeting the von Hippel-Lindau E3 ubiquitin ligase using small molecules to disrupt the VHL/HIF-1alpha interaction. J. Am. Chem. Soc 2012, 134, 4465–4468. [PubMed: 22369643]

(48). Buckley DL; Gustafson JL; Van Molle I; Roth AG; Tae HS; Gareiss PC; Jorgensen WL; Ciulli A; Crews CM Small-molecule inhibitors of the interaction between the E3 ligase VHL and HIF1alpha. Angew. Chem., Int. Ed 2012, 51, 11463–11467.

(49). Buckley DL; Raina K; Darricarrere N; Hines J; Gustafson JL; Smith IE; Miah AH; Harling JD; Crews CM HaloPROTACS: use of small molecule PROTACs to induce degradation of HaloTag fusion proteins. ACS Chem. Biol 2015, 10, 1831–1837. [PubMed: 26070106]

(50). Fischer ES; Bohm K; Lydeard JR; Yang H; Stadler MB; Cavadini S; Nagel J; Serluca F; Acker V; Lingaraju GM; Tichkule RB; Schebesta M; Forrester WC; Schirle M; Hassiepen U; Ottl J; Hild M; Beckwith RE; Harper JW; Jenkins JL; Thoma NH Structure of the DDB1-CRBN E3 ubiquitin ligase in complex with thalidomide. Nature 2014, 512, 49–53. [PubMed: 25043012]

(51). Fabian MA; Biggs WH 3rd; Treiber DK; Atteridge CE; Azimioara MD; Benedetti MG; Carter TA; Ciceri P; Edeen PT; Floyd M; Ford JM; Galvin M; Gerlach JL; Grotzfeld RM; Herrgard S; Insko DE; Insko MA; Lai AG; Lelias JM; Mehta SA; Milanov ZV; Velasco AM; Wodicka LM; Patel HK; Zarrinkar PP; Lockhart DJ A small molecule-kinase interaction map for clinical kinase inhibitors. Nat. Biotechnol 2005, 23, 329–336. [PubMed: 15711537]

(52). Douglass EF Jr; Miller CJ; Sparer G; Shapiro H; Spiegel DA A comprehensive mathematical model for three-body binding equilibria. J. Am. Chem. Soc 2013, 135, 6092–6099. [PubMed: 23544844]

(53). Tan X; Thapa N; Sun Y; Anderson RA A kinase-independent role for EGF receptor in autophagy initiation. Cell 2015, 160, 145–160. [PubMed: 25594178]

(54). Soucy TA; Smith PG; Milhollen MA; Berger AJ; Gavin JM; Adhikari S; Brownell JE; Burke KE; Cardin DP; Critchley S; Cullis CA; Doucette A; Garnsey JJ; Gaulin JL; Gershman RE; Lublinsky AR; McDonald A; Mizutani H; Narayanan U; Olhava EJ; Peluso S; Rezaei M; Sintchak MD; Talreja T; Thomas MP; Traore T; Vyskocil S; Weatherhead GS; Yu J; Zhang J; Dick LR; Claiborne CF; Rolfe M; Bolen JB; Langston SP An inhibitor of NEDD8-activating enzyme as a new approach to treat cancer. Nature 2009, 458, 732–736. [PubMed: 19360080]

(55). Frost J; Galdeano C; Soares P; Gadd MS; Grzes KM; Ellis L; Epemolu O; Shimamura S; Bantscheff M; Grandi P; Read KD; Cantrell DA; Rocha S; Ciulli A Potent and selective chemical probe of hypoxic signalling downstream of HIF-alpha hydroxylation via VHL inhibition. Nat. Commun 2016, 7, No. 13312.

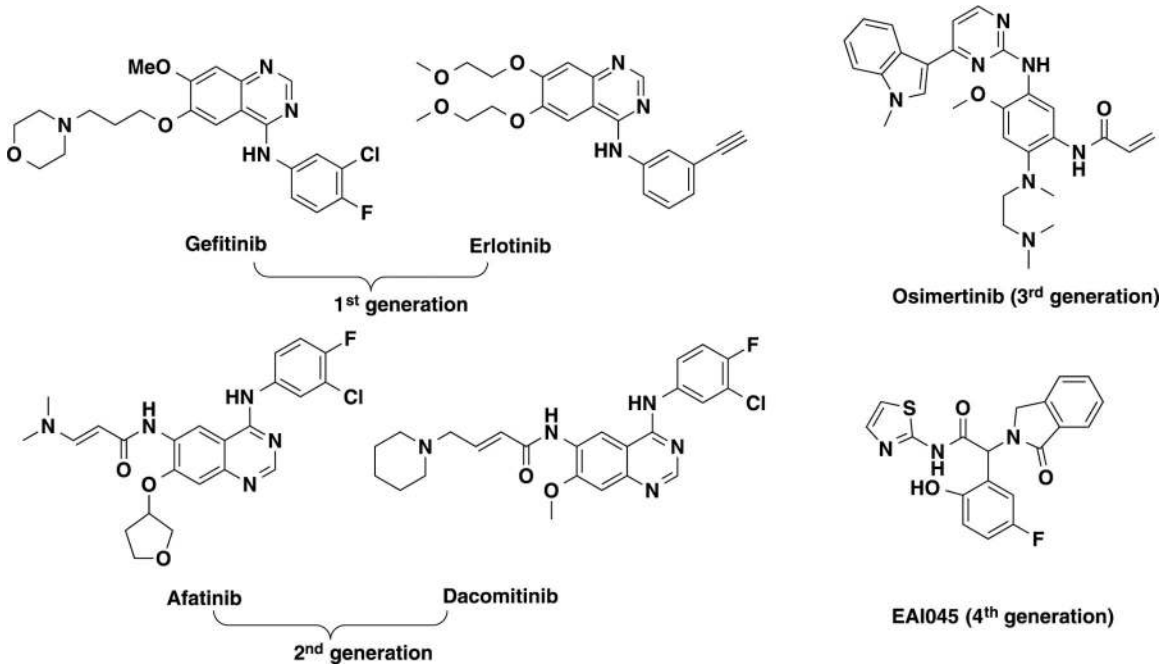

Figure 1.
Chemical structures of representative first-, second-, third-, and fourth-generation EGFR TKIs.

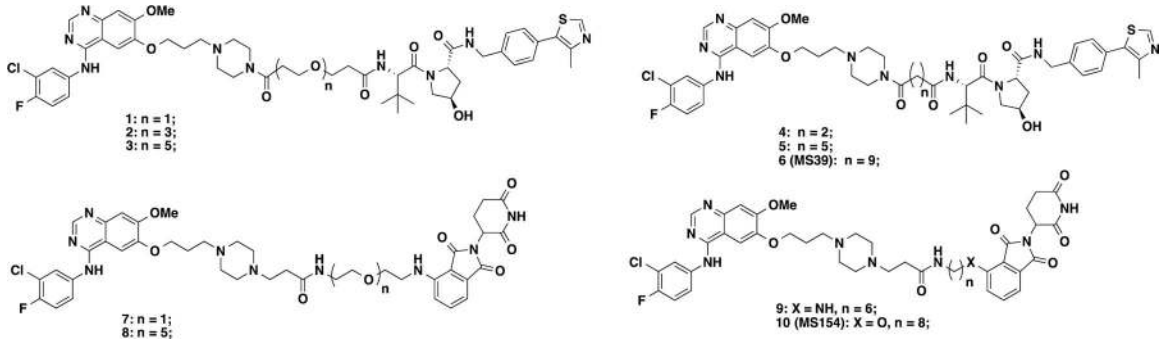

Figure 2.
Chemical structures of designed gefitinib-based EGFR degraders **1–10**.

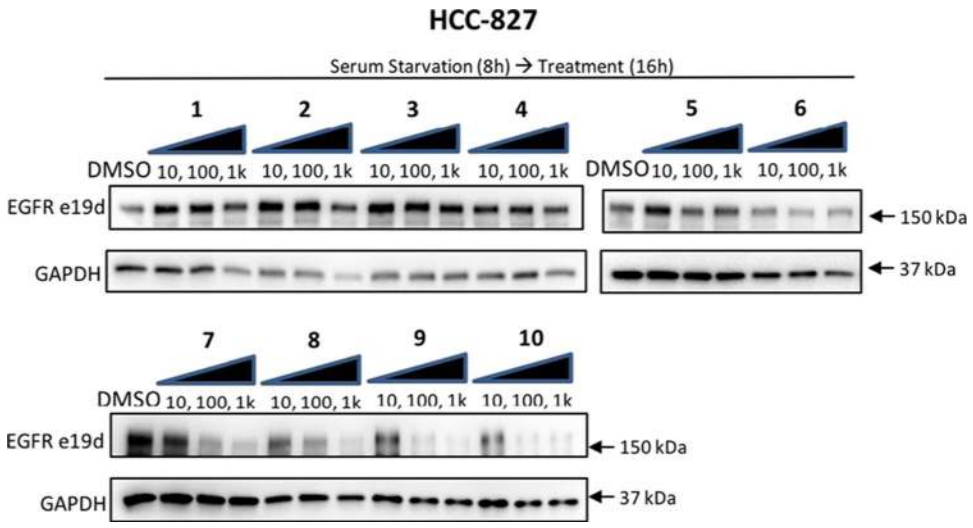

Figure 3.

Western blotting analysis of EGFR protein in HCC-827 cells treated with compounds **1–10**. (A) VHL-1-based compounds **1–6** and (B) CRBN-based compounds **7–10** were tested in HCC-827 cell lines using three different concentrations (10, 100, and 1000 nM). EGFR e19d: EGFR mutant with exon 19 deletion.

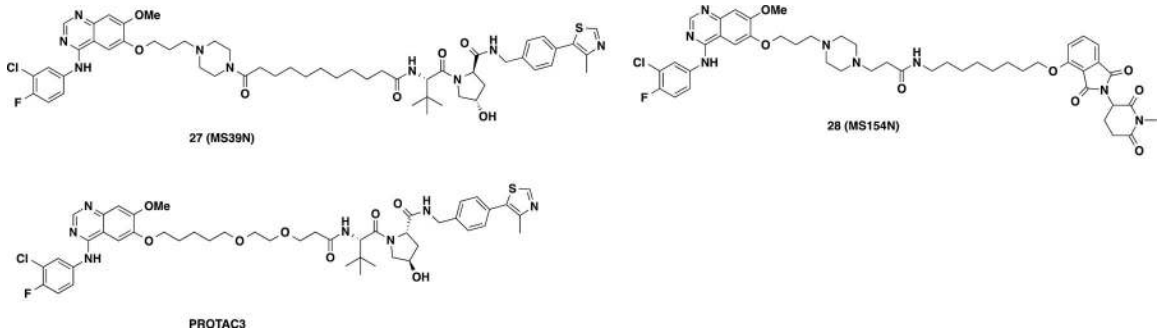

Figure 4.

Chemical structures of compounds **27** and **28** and the previously reported EGFR degrader PROTAC3.

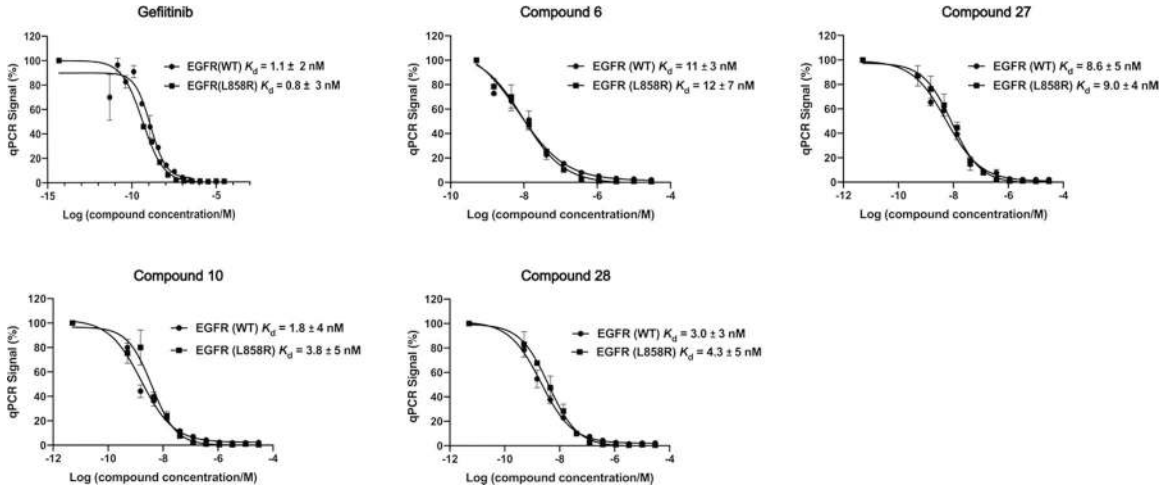

Figure 5.

Compounds **6**, **27**, **10**, and **28** bind EGFR WT and L858R mutants with high affinities. The K_d determinations were performed in a competitive binding assay in duplicate. Error bars represent ± standard error of the mean (SEM) in duplicated independent experiments.

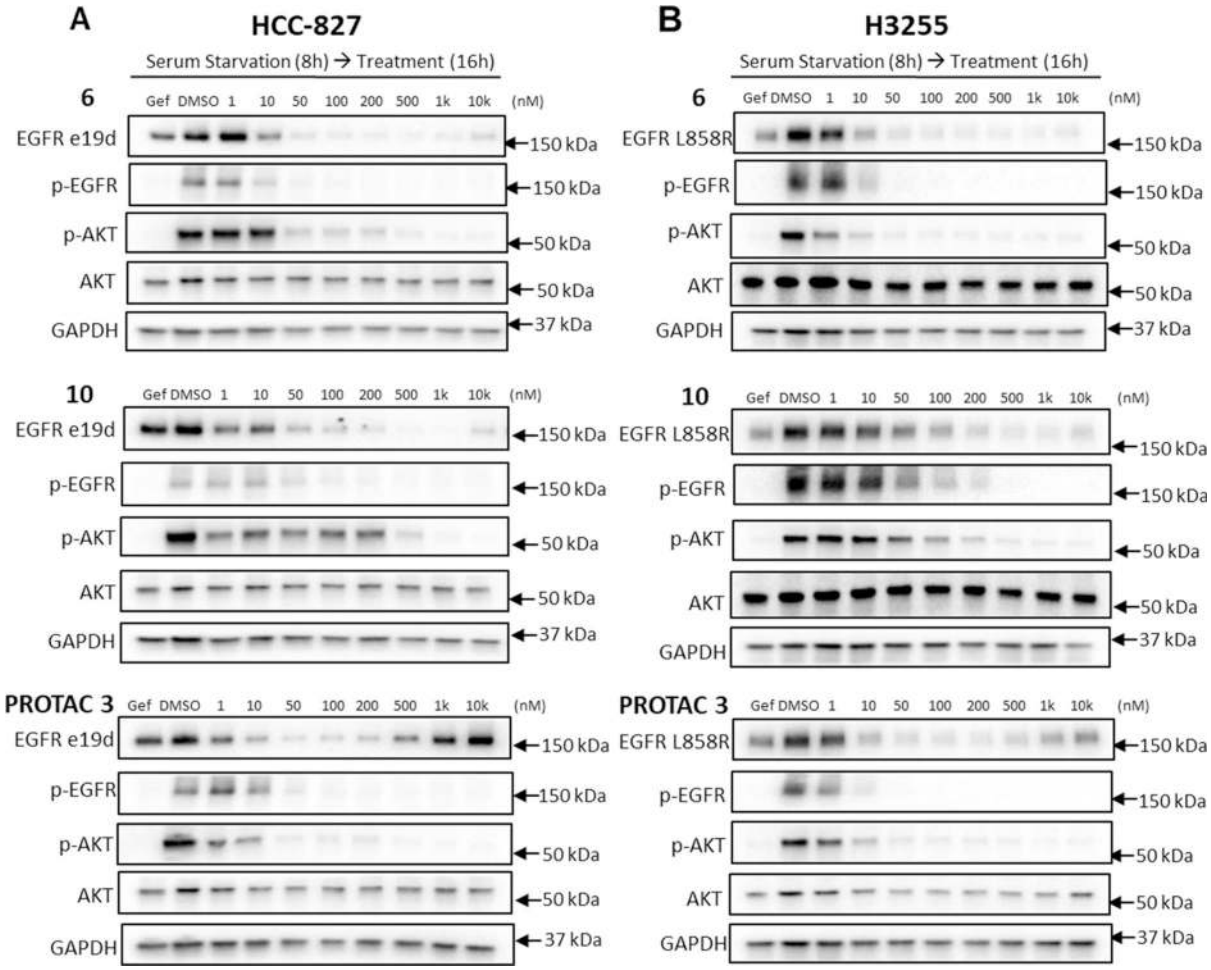

Figure 6.

Compounds **6** and **10** potently reduced protein levels of EGFR mutants and inhibited downstream signaling in lung cancer cells. NSCLC cell lines HCC-827 (A) and H3255 (B) were cultured to 80% confluent and then switched to a serum-free medium for 8 h before treating with indicated concentrations of the compounds for another 16 h. EGFR e19d: EGFR mutant with exon 19 deletion; EGFR L858R: EGFR L858R single point mutant; Gef: gefitinib (parental EGFR inhibitor; 1 μM); 1k: 1000; 10k: 10 000.

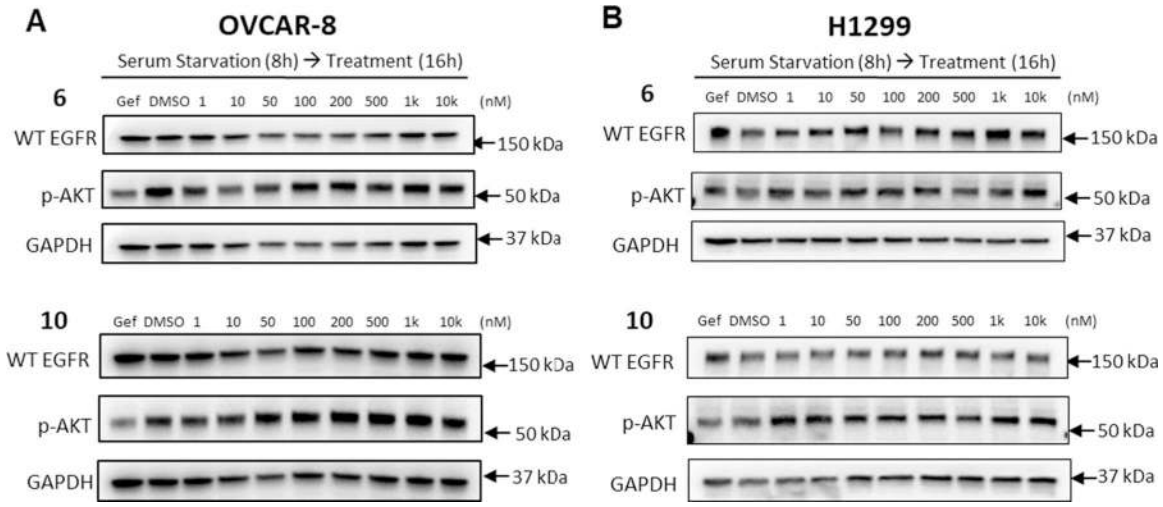

Figure 7.

Compounds **6** and **10** did not significantly reduce WT EGFR protein levels in OVCAR-8 (**A**) and H1299 (**B**) cells. OVCAR-8 and H1299 cells were cultured to 80% confluent and then switched to a serum-free medium for 8 h before treating with indicated concentrations of the compounds for another 16 h. Gef: gefitinib (1 μM).

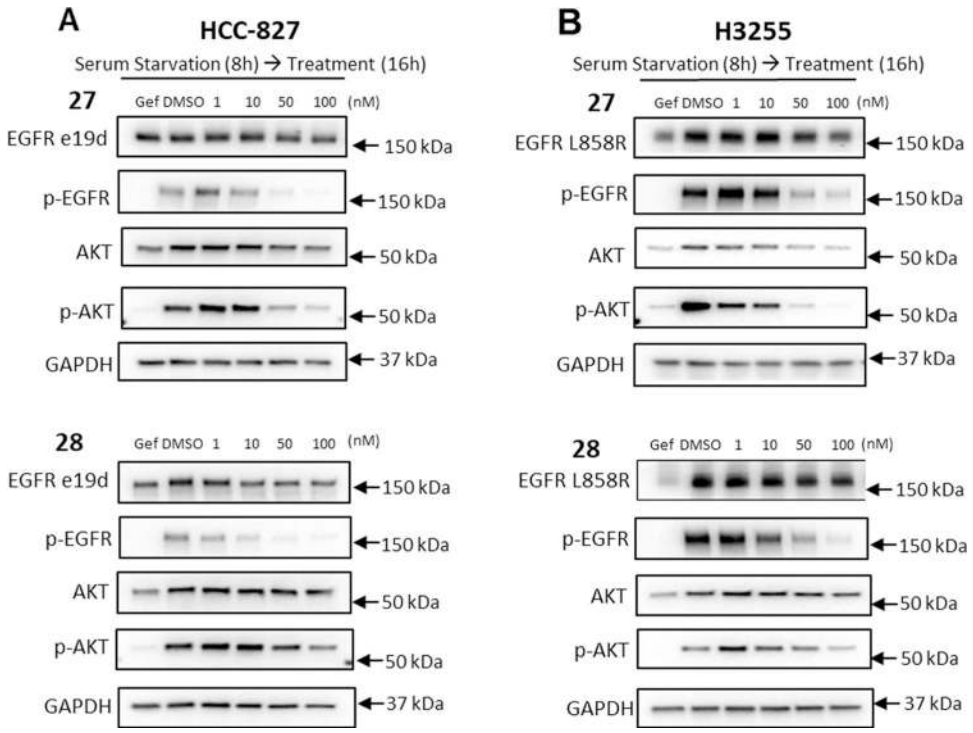

Figure 8.

Compounds **27** and **28** did not significantly reduce the protein levels of EGFR mutants in HCC-827 and H3255 cells. HCC-827 (A) and H3255 (B) cells were cultured to 80% confluent and then switched to a serum-free medium for 8 h before treating with indicated concentrations of the compounds for another 16 h.

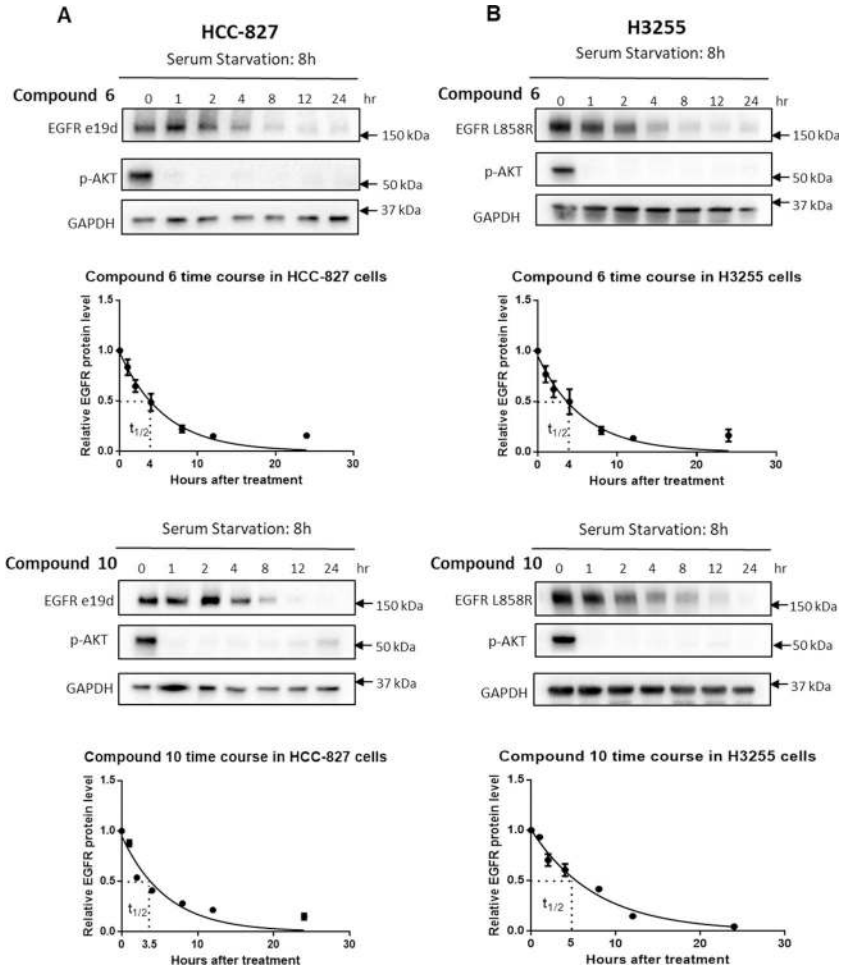

Figure 9.

Compounds **6** and **10** rapidly and time-dependently elicit the degradation of EGFR mutants in lung cancer cells. A final concentration of 100 nM compound **6** or **10** was added to HCC-827 cells (A) and H3255 cells (B) after 8 h of serum starvation. At each time point, cells were collected for Western blot. The time needed for the degradation of 50% protein ($t_{1/2}$) was determined by the intensity of Western bands and normalized to GAPDH. Error bars represent the standard errors in three independent experiments.

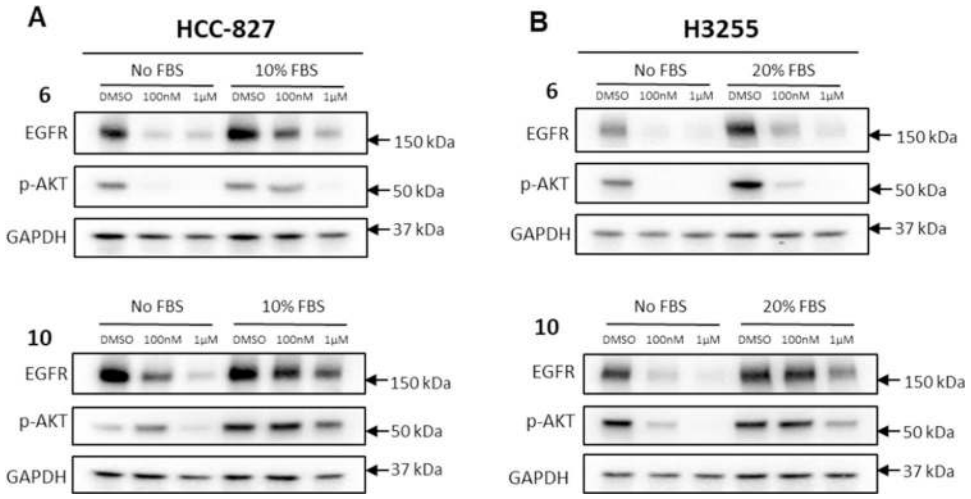

Figure 10.

Serum starvation enhances the EGFR degradation induced by compounds **6** and **10**. Cultured HCC-827 cells (A) and H3255 cells (B) were switched to a serum-free/serum-containing medium for 8 h and then treated with the indicated concentrations of the degraders for 16 h.

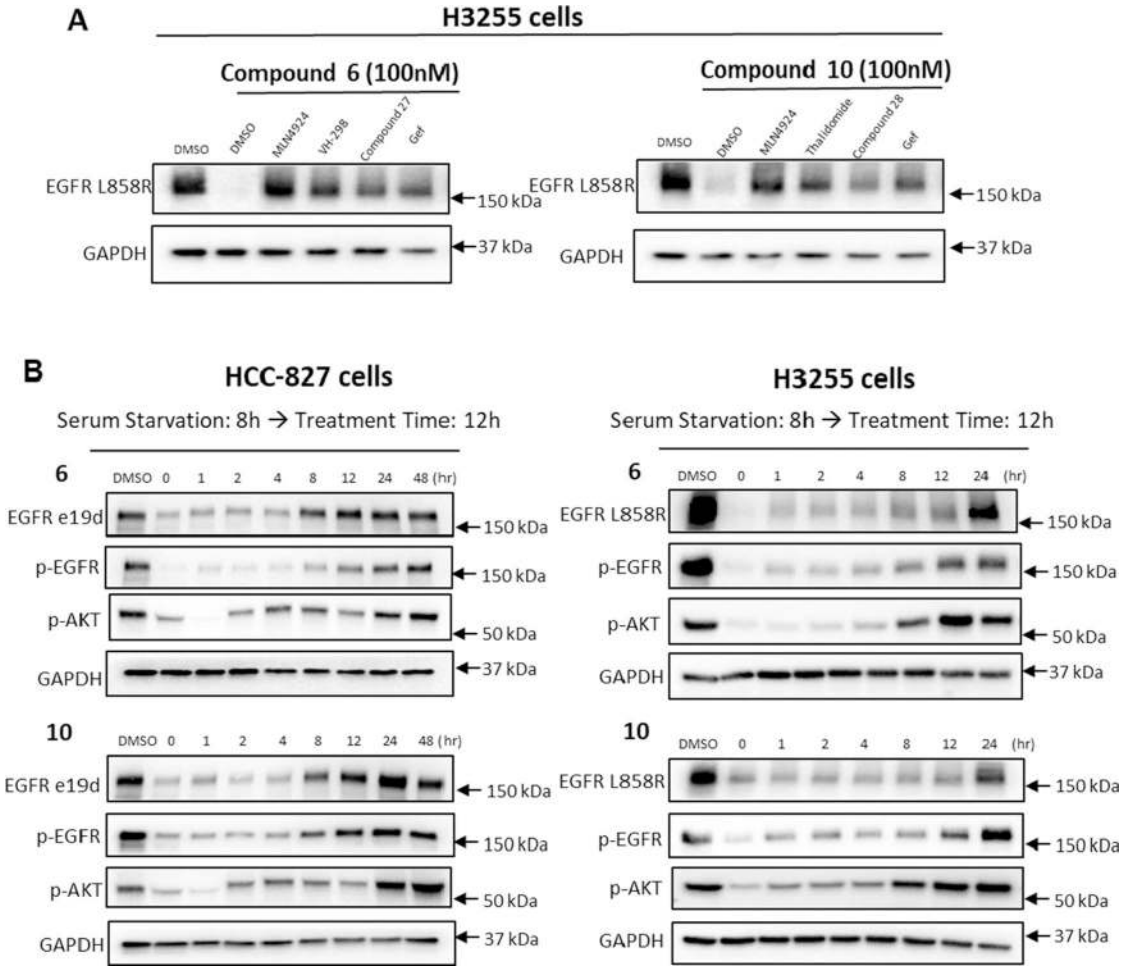

Figure 11.

EGFR degradation effect of compounds **6** and **10** is mediated through the E3 ubiquitin ligase components VHL and CRBN, respectively, and is reversible upon washout. (A) H3255 cells were starved for 4 h and then pretreated with the indicated chemicals for 2 h before degrader (100 nM) treatment for another 8 h. The final concentrations of the compounds used for pretreatment are DMSO (0.1% v/v), MLN4924 (1 μM), VH-298 (10 μM), thalidomide (10 μM), negative controls (compound **27** for degrader **6** and compound **28** for degrader **10**, 10 μM), and gefitinib (10 μM). (B) HCC-827 and H3255 cells were starved for 8 h before a 12 h degrader treatment, then washed with PBS three times, and harvested at the indicated time points for Western blot analysis.

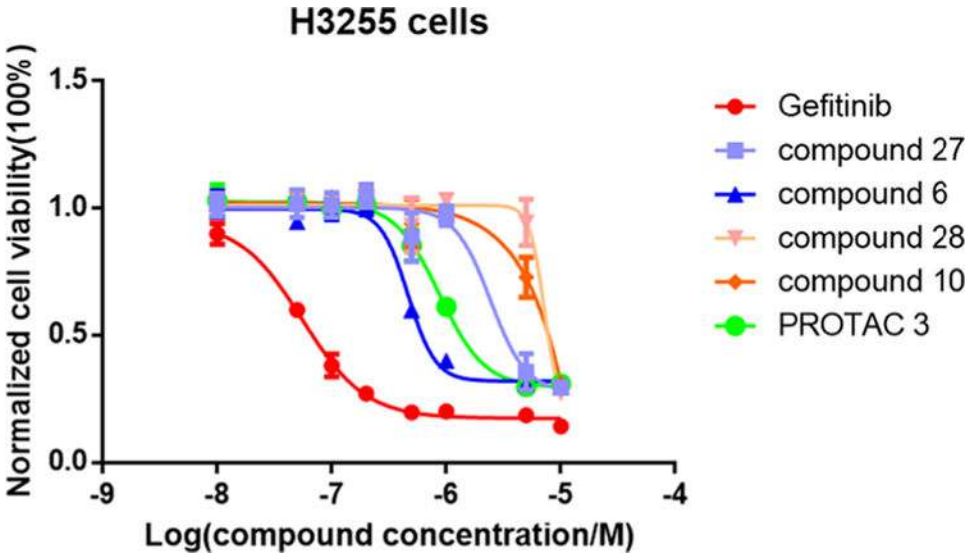

Figure 12.

Compounds **6** and **10** inhibit the proliferation of lung cancer H3255 cells. H3255 cells were seeded to 96-well plates a night before at 4000 cells/well and then treated with serial dilutions of degraders or controls for 3 days. Cell number/growth was measured using Cell Counting Kit-8 and error bars indicating the standard errors in three independent experiments.

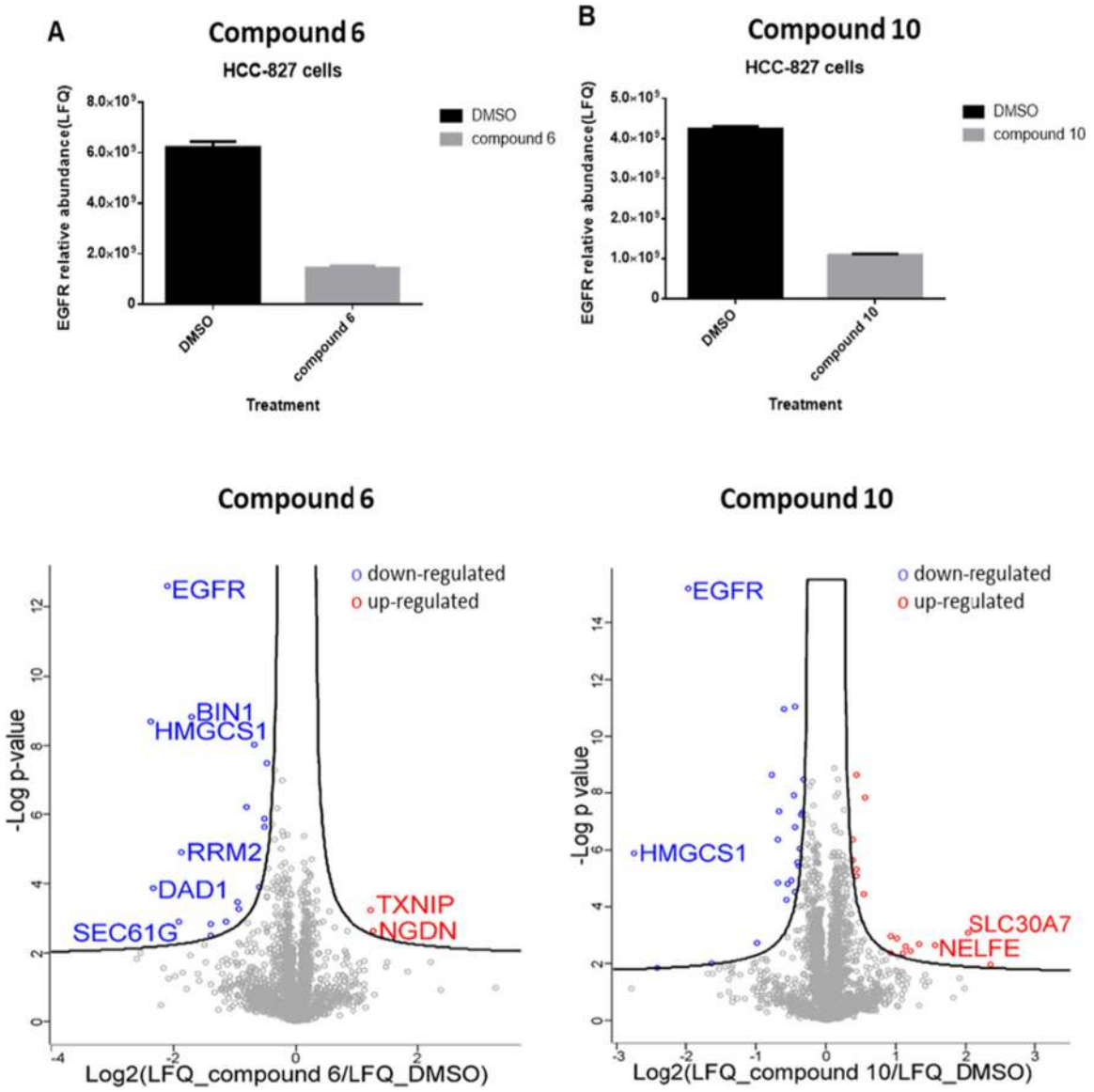

Figure 13.

Global proteomic analyses indicate that compounds **6** and **10** are highly selective EGFR degraders. HCC-827 cells were starved for 8 h and treated with compound **6** (A) or compound **10** (B) at 100 nM for 16 h and then collected for liquid chromatography–mass spectrometry (LC–MS) analyses. Label-free quantification (LFQ) was used to calculate peptide intensity; the top panels showed the relative abundance of EGFR (LFQ intensity value) between the degrader-treated and control groups. Error bars indicate the standard errors in three independent experiments.

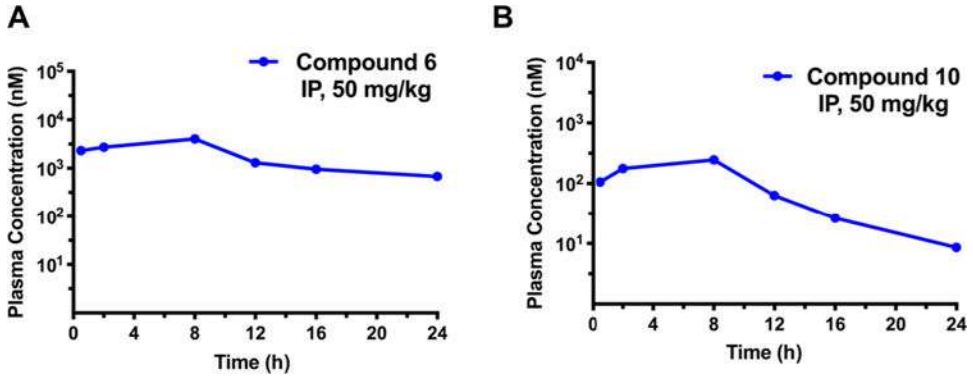

Figure 14.

EGFR degraders **6** and **10** are bioavailable in mouse PK studies. Plasma concentrations of compound **6** (A) and compound **10** (B) following a single 50 mg/kg IP injection over 24 h in male Swiss Albino mice. Experiments were carried out in biological triplicates, with points representing mean concentrations ± SEM.

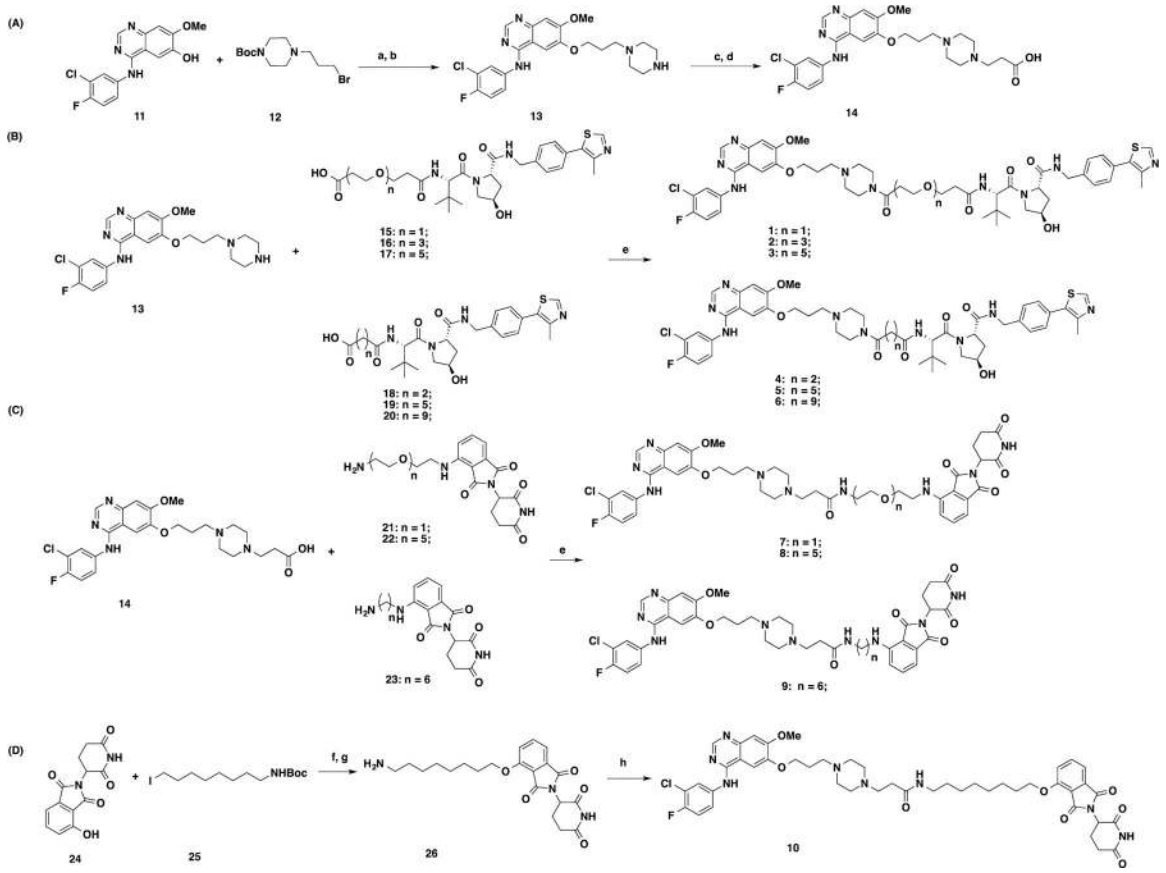

Scheme 1.

Synthesis of Gefitinib-Based EGFR Degraders 1–10[a]

[a]Reaction conditions: (a) K_2CO_3, dimethylformamide (DMF), 80 °C; (b) trifluoroacetic acid (TFA), dichloromethane (DCM), room temperature (rt), 30 min; (c) ethyl 3-bromopropanoate, K_2CO_3, DMF, 80 °C; (d) LiOH, tetrahydrofuran (THF), H_2O, rt, 12 h; (e) 1-ethyl-3-(3-dimethylaminopropyl)carbodiimide (EDCI), 1-hydroxy-7-azabenzo-triazole (HOAt), *N*-methylmorpholine (NMM), dimethyl sulfoxide (DMSO), rt, 4 h; (f) $NaHCO_3$, NaI, DMF, 65 °C, 2 days; (g) TFA/DCM, rt, 30 min; (h) 14, EDCI, HOAt, NMM, DMSO, rt, 12 h.

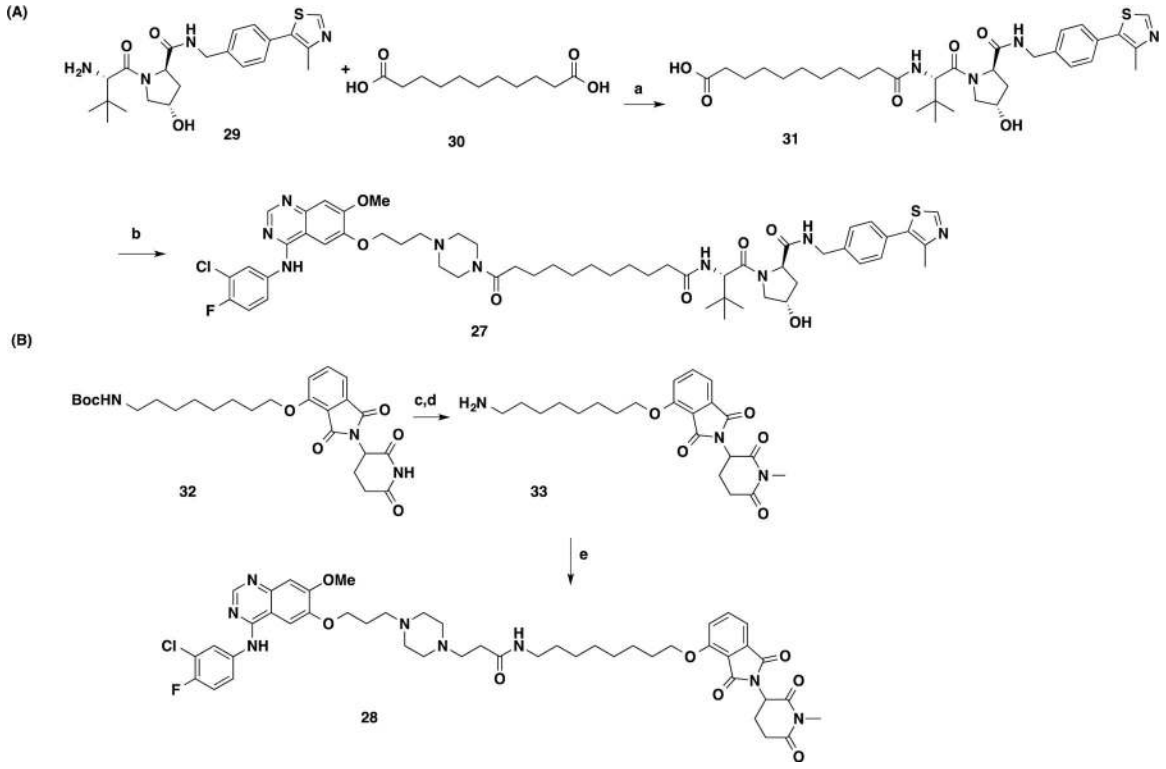

Scheme 2.

Synthesis of Negative Control Compounds 27 and 28[a]

[a]Reaction conditions: (a) 1-ethyl-3-(3-dimethylaminopropyl)carbodiimide (EDCI), 1-hydroxy-7-azabenzo-triazole (HOAt), N-methylmorpholine (NMM), dimethyl sulfoxide (DMSO), rt, 4 h; (b) 13, EDCI, HOAt, NMM, DMSO, rt, 12 h; (c) K_2CO_3, CH_3I, DMF, rt, 4 h; (d) TFA/DCM, rt, 30 min; (e) 14, EDCI, HOAt, NMM, DMSO, rt, 12 h.